

Scientific Programme

ABSTRACTS

ORAL PRESENTATIONS

ESSR 2004

June 18 – 19, 2004

Augsburg, Germany

www.essr.org

Oral Presentations

I. Trauma and Related Topics Friday, 08:00 – 10:00

Welserszimmer

Chairperson: Obermann W, Leiden, The Netherlands

- 08:00 MR IMAGING IN CHANCE-TYPE FLEXION DISTRACTION (CTFD) SPINAL INJURIES
p9 Groves C, Cassar-Pullicino V. Oswestry, United Kingdom
- 08:10 DEVELOPMENT OF A LOW DOSE MULTI-SLICE CT (MSCT) SCANNING PROTOCOL FOR USE IN
p10 SPINAL TRAUMA
Krolak C, Linsenmaier U, Coppentrath E, Pfeifer KJ, Reiser M. München, Germany
- 08:20 MR SIGNAL ALTERATIONS IN THE ACUTE ONSET OF HETEROTOPIC OSSIFICATION IN
p11 PATIENTS WITH SPINAL CORD INJURY
Ledermann HP, Berger MF, Knecht H, Wick LF. Basel, Switzerland
- 08:30 NON POST-RADIOTHERAPY PELVIC RING INSUFFICIENCY FRACTURES: DON'T MISS
p12 ASSOCIATED INJURIES
Llopis E, Higuera V, Ferrer P, Munoz I, Trenor P, Martinez A. Valencia, Spain
- 08:40 AVASCULAR OSTEONECROSIS OF THE PROXIMAL FRAGMENT IN SCAPHOID NONUNION:
p13 IS INTRAVENOUS APPLICATION OF CONTRAST AGENT REALLY NECESSARY?
Schmitt R, Coblenz G, Fröhner S, Megele K, Krimmer H, Christopoulos G. Bad Neustadt/Saale, Germany
- 08:50 COMPARISON BETWEEN 16 DETECTOR MULTISLICE CT AND SKELETAL SCINTIGRAPHY IN
p14 THE DIAGNOSIS OF OCCULT SCAPHOID FRACTURES: DISCRIMINATIVE VALUE OF
QUANTIFICATION OF ^{99m}Tc-MDP UPTAKE
Groves AM, Cheow HK, Bearcroft PWP, Coleman M, Wood H, Balan KK, Dixon AK. Oxford, United Kingdom
- 09:00 FRACTURES OF THE TOP OF THE GREATER TROCHANTER AT RADIOGRAPHY AND ITS
p15 ASSOCIATION TO AN INTRA-TROCHANTERIC FRACTURE AS DEMONSTRATED BY MR
IMAGING: DISCUSSION OF CLINICAL AND SURGICAL CONSEQUENCES
Gelineck J, Andersen K, Egund N. Aarhus, Denmark
- 09:10 EVALUATION OF ORGAN DOSES AND EFFECTIVE DOSE FOR PELVIC AND LUMBAR SPINE
p16 EXAMINATIONS USING A C-ARM BASED CT-SYSTEM IN COMPARISON TO A SINGLE SLICE
CT
Fischer T, Linsenmaier U, Kotsianos D, Wirth S, Goldbrunner H, Pfeifer KJ, Reiser M. München, Germany
- 09:20 MULTIDETECTOR ROW CT VERSUS DIGITAL RADIOGRAPHY IN THE EVALUATION OF BONE
p17 HEALING IN ORTHOPEDICS PATIENTS
Krestan CR, Noske H, Vasilevska E, Schuller G, Czerny C, Imhof H. Wien, Austria
- 09:30 ACCURACY OF COMPUTER-ASSISTED PIN PLACEMENT USING A FLUOROSCOPY GUIDED
p18 NAVIGATION SYSTEM AND A NOVEL TARGETING DEVICE: A PHANTOM STUDY
Bale RJ, Kovacs P, Lang T, Knoflach M, Rosenberger RE, Hoser C, Blauth M, Jaschke W. Innsbruck, Austria
- 09:40 ULTRASOUND EVALUATION OF PECTORAL MUSCLE INJURIES
p19 Rehman A, Robinson P. Leeds, United Kingdom
- 09:50 KNEE JOINT 3D MODEL RECONSTRUCTED WITH CT AND MRI IMAGES: AN INNOVATIVE
p20 CONCEPT FOR BIOMECHANICAL STUDY OF BONE AND SOFT STRUCTURES
Ramaniraka NA, Siegrist O, Terrier A, Theumann N. Lausanne, Switzerland
- 10:00 Coffee Break

Chairperson: Link T, San Francisco, USA

10:30 QUANTITATIVE COMPUTED TOMOGRAPHY IN THE EVALUATION OF
p21 BONE DENSITY IN CHILDREN

Alzen G, Berthold D, Moritz D. Gießen, Germany

10:40 IDENTIFICATION OF OSTEOPOROTIC VERTEBRAL FRACTURES IN
p22 POSTMENOPAUSAL FEMALES ON LATERAL CHEST RADIOGRAPHS

Calleja M, Chasi I, Hide G. Newcastle, United Kingdom

10:50 DIAGNOSIS OF OSTEOPOROSIS: VISUAL ASSESSMENT OF
p23 CONVENTIONAL AND DIGITAL RADIOGRAPHY IN COMPARISON
WITH DUAL X-RAY ABSORPTIOMETRY OF THE LUMBAR SPINE

Baur-Melnyk A, Stäbler A, Sittek H, Bonel H, Laeverenz G, Reiser M.
München, Germany

11:00 VERTEBRAL ASSESSMENT BY PLAIN X-RAYS FILM: ACCURACY AND
p24 PRECISION OF AN AUTOMATIC SOFTWARE

Guglielmi G, Brett A, Haslam J, Walker K, Placentino MG, Catalano F.
San Giovanni Rotondo, Italy

11:10 THE INFLUENCE OF POSTERIOR INSTRUMENTATION ON ADJACENT
p26 AND TRANSFIXED FACET JOINTS IN PATIENTS WITH
THORACOLUMBAR SPINAL INJURIES: A MORPHOLOGICAL IN VIVO
STUDY USING COMPUTED TOMOGRAPHY OSTEOABSORPTIOMETRY

Wagner S, Müller-Gerbl M, Weckbach A. München, Germany

11:20 HARRIS LINES OF THE TIBIA ACROSS CENTURIES: A COMPARISON OF
p28 TWO POPULATIONS, MEDIEVAL AND CONTEMPORARY IN CENTRAL
EUROPE

Ameen S, Staub L, Ballmer F, Ulrich S, Vock P, Anderson SE. Bern, Switzerland

11:30 STUDY TO DESCRIBE THE MORPHOLOGY OF A SERIES OF CLAVICLES
p29 & THE DIMENSIONS OF ITS INTRAMEDULLARY CANAL

Ahmad M, Trewhella MJ, Bayliss NC. Stockton, United Kingdom

11:45 OPENING CEREMONY

Mozartsaal

**III. Sonographic Diagnosis and Intervention in the
Musculoskeletal System**
Friday, 13:30 – 15:10

Welserszimmer

Chairperson: McNally E, Oxford, United Kingdom

- 13:30 ULTRASOUND ASSESSMENT OF EARLY CLUBFOOT TREATMENT
p30 Aurell Y., Andriess H, Johansson A, Jonsson K. Halmstad, Sweden
- 13:40 COMPLETE AND INCOMPLETE FINGER PULLEY DISRUPTION: HR-US EVALUATION
p31 IN A CADAVER MODEL
Bodner G., Bernathova M, Rasp M, Kovacs P, Kamelger F, Gabl M. Innsbruck, Austria
- 13:50 SYMPTOMATIC PROXIMAL PATELLAR TENDINOSIS: CORRELATION BETWEEN
p32 POWER DOPPLER ULTRASONOGRAPHY (PDU) AND CLINICAL SEVERITY
Brys P., Geusens E, Van Breuseghem I, Van Cleynenbreugel J, Peers K, Bellemans J. Leuven, Belgium
- 14:00 THE USEFULNESS OF ULTRASOUND IN THE ASSESMENT OF ACUTE ACHILLES
p33 TENDON RUPTURE
David S., Ostlere S. Oxford, United Kingdom
- 14:10 ULTRASONOGRAPHIC EXAMINATION OF ACHILLES TENDON IN THE ITALIAN
p34 RUGBY TEAM PLAYERS
Parodi S., Spagnolo P, Pastorino R, Falchi M, Silvestri E, Garlaschi G. Genova, Italy
- 14:20 USEFULNESS OF ULTRASONOGRAPHY IN THE DIAGNOSIS OF CARPAL TUNNEL
p35 SYNDROME
Pinilla I, Martin-Hervás C, Bernabéu D., Santiago S, Gómez-Bajo G. Madrid, Spain
- 14:30 PERCUTANEUS MANAGEMENT OF CHRONIC CALCIFIC TENDINITIS OF THE
p36 SHOULDER
Zabala R., Del Cura JL, Legórburu A, Torre I, Garcia A, Grande D. Bilbao, Spain
- 14:40 THE USE OF ULTRASOUND GUIDED ASPIRATION / BIOPSY IN SPINAL PATHOLOGY
p37 Elliott JM., Grey AC, Davis RI. Belfast, United Kingdom
- 14:50 ULTRASOUND-GUIDED PERCUTANEOUS NEEDLE THERAPY OF THE ELBOW
p38 EPICONDYLITIS
Obradov M., Eygendaal D, Anderson PG, Reijnierse M. Nijmegen, The Netherlands
- 15:00 USE OF CURAVISC IN KNEE DISORDER – ULTRASOUND REPORT
p39 Djokic B., Stankovic B. Nis, Serbia & Montenegro
- 15:15 Coffee Break

IV. Rheumatology, Osteoarthritis

(In Cooperation with Rheumatology Subcommittee of the
ESSR.)

Fuggerzimmer

Friday, 15:45 – 17:35

Chairperson: Egund N, Aarhus, Denmark

- 15:45 QUANTIFICATION OF ARTHRITIS WITH PLAIN FILM RADIOGRAPHY
p40 Kainberger F. Wien, Austria
- 15:55 US AND MR ASSESMENT OF SYNOVITIS
--- Grainger A. Leeds, United Kingdom
- 16:05 US AND MR ASSESSMENT OF EROSIONS
--- O'Connor P. Leeds, United Kingdom
- 16:15 QUANTIFICATION OF SACROILIITIS BY MRI
--- Egund N. Jurik A. Aarhus, Denmark
- 16:25 THE EULAR-OMERACT MRI IN RHEUMATOID ARTHRITIS REFERENCE FILM ATLAS –
p41 A NEW TOOL FOR STANDARDIZED ASSESSMENT OF RHEUMATOID JOINT
INFLAMMATION AND DESTRUCTION
Ostergaard M. Bird P, McQueen F, Ejbjerg B, Edmonds J, Lassere M, Peterfy C, O'Connor P,
Shnier R, Genant H, Emery P, Conaghan P. Copenhagen, Denmark
- 16:35 MAGNETIC RESONANCE IMAGING IDENTIFIES SUBCLINICAL FEATURES THAT
p42 PREDICT EXTENSION OF ARTHRITIS IN CHILDREN WITH OLIGOARTHRTIS
Johnson K. Gardner-Medwin J, Ryder CAJ. Birmingham, United Kingdom
- 16:45 A PILOT STUDY FOR THE VISUALIZATION AND ANALYSIS OF ARTHRITIC CHANGES
p43 IN THE RAT KNEE JOINT BY MICRO CT ARTHROGRAPHY
Roemer FW. Mohr A, Lynch JA, Meta MD, Guermazi A, Genant HK. Augsburg, Germany
- 16:55 ACHILLES TENDON ENTHESOPATHY IN PSORIASIS: DIAGNOSTIC IMAGING WITH
p44 COMPARISON BETWEEN SONOGRAPHY, COLOR-DOPPLER AND MAGNETIC
RESONANCE
Maggi F. Di Gregorio F, De Simone C. Roma, Italy
- 17:05 MAGNETIC RESONANCE IMAGING IN KNEES OF PATIENTS WITH OSTEOARTHRTIS
p45 AT MULTIPLE SITES: ASSOCIATION WITH CLINICAL FINDINGS
Kornaat PR. Bloem JL, Ceulemans RYT, Riyazi N, Rosendaal FR, Nelissen RG, Kloppenburg M.
Leiden, The Netherlands
- 17:15 DIAGNOSTIC IMPACT OF HIGH RESOLUTION COMPUTED TOMOGRAPHY (HRCT) IN
p46 THE ELBOW
Mester A. Nemeth L, Kakosy T, Posgay M, Karlinger K, Mako E. Budapest, Hungary
- 17:25 IMAGE QUALITY IN THE LATEST DEVELOPMENT OF DIGITAL RADIOGRAPHY:
p47 ASSESSMENT AND COMPARISON AT CR AND DR OF SMALL JOINTS
Loft L. Jurik A, Rasmussen J, Jensen JJ, Egund N. Aarhus, Denmark

Chairperson: Adam G, Hamburg, Germany

- 08:30
p48 COMPARISON OF IONIC AND NON-IONIC CONTRAST AGENTS FOR
CONTRAST-ENHANCED MR IMAGING OF PROTEOGLYCAN DEPLETED
ARTICULAR CARTILAGE
Wiener E, Wörtler K, Settles M, Rummeny EJ. München, Germany
- 08:40
p49 HIGH RESOLUTION DIFFUSION TENSOR IMAGING OF ARTICULAR
CARTILAGE
Glaser C, Filidoro L, Dietrich O, Oerther T, Witt M, Weber J, Reiser M.
München, Germany
- 08:50
p50 IMAGING OF ADVANCED ARTICULAR CARTILAGE DISEASE USING 3D
SPGR,
3D CISS AND PROTON FSE IMAGING AND ARTHROSCOPIC CORRELATION
Gur S, Arkun R, Aydogdu S, Argin M. Izmir, Turkey
- 09:00
p51 THE MEASUREMENT OF ARTICULAR CARTILAGE THICKNESS IN THE WRIST
van der Leij C, Streekstra GJ, Strackee S, Maas M. Amsterdam, The Netherlands
- 09:10
p52 CARTILAGE DAMAGE AND SYNOVIUM CHANGES IN HAEMOPHILIC
ARTHROPATHY: EVALUATION WITH MAGNETIC RESONANCE IMAGING
Fotiadis NI, Girtovitis FI, Haritanti A, Dimitriadis AS, Makris PE. Thessaloniki, Greece
- 09:20
p53 MRI IN MEMBRANOUS AUTOLOGOUS CHONDROCYTE IMPLANTATION
(MACI)
Fontoira E, Sánchez E, Padrón M. Madrid, Spain
- 09:30
p54 ARTHRO-MRI VIRTUAL ENDOSCOPY OF THE SHOULDER: PRELIMINARY
RESULTS
Di Pietro M, Lelli S, Calvisi V, Barile A, Masciocchi C. L'Aquila, Italy
- 09:40
p55 DOES MARATHON RUNNING CAUSE STRESS ON THE KNEE WHICH IS
DEMONSTRABLE ON MR IMAGING?
Weidekamm C, Uffmann M, Schueller G, Bader T. Wien, Austria
- 09:50
p56 MR ACCESSORY CLEFT SIGN IN THE DIAGNOSIS OF GROIN PAIN
Cunningham PM, Brennan D, O'Brien J, O'Neill P, Eustace S. Dublin, Ireland
- 10:00 Coffee Break

VI. Tumors, Tumor-like Lesions, Osteodysplasia

Saturday, 10:30 – 12:00

Welserszimmer

Chairperson: Anderson S, Bern, Switzerland

10:30 POLYCYSTIC LIPOMEMBRANOUS OSTEODYSPLASIA WITH
p57 SKLEROSING LEUKENCEPHALOPATHY (NASU-HAKOLA DISEASE) – 5
NEW CASES –

Freyschmidt J, Sternberg A, Wiens J, Madry H. Bremen, Germany

10:40 NORA'S LESION, A DISTINCT RADIOGRAPHIC ENTITY?
p58 Dhondt E, Oudenhoven L, Kroon H, Nieborg A, Hoogendoorn P, Bloem JL,
De Schepper A. Leiden, The Netherlands

10:50 GIANT CELL TUMOR OF THE TENDON SHEATH OF THE HAND:
p59 MR FINDINGS

Ortori S, Zampa V, Giusti S, Vagli P, Odoguardi F, Alfieri P, Bartolozzi C.
Pisa, Italy

11:00 THE VALUE OF THE „FLOW-VOID SIGN“ ON MRI OF OSSEOUS
p60 METASTASES FROM RENAL CELL CARCINOMA

Allen G, Davies AM, Grimer RJ. Birmingham, United Kingdom

11:10 WHOLE BODY MSCT VERSUS WHOLE BODY MRI IN DIAGNOSTICS OF
p61 MULTIPLE MYELOMA

Wieser A, Baur A, Reiser M. München, Germany

11:20 PREOPERATIVE MONITORING OF NEOADJUVANT THERAPY IN SOFT
p62 TISSUE SARCOMAS: THE EFFICACY AND LIMITATIONS OF MRI

Memis Oktay A, Arkun R, Argin M, Akalin T, Anacak Y, Arun S. Izmir, Turkey

11:30 BENEFIT OF PEER REVIEWED PATHOLOGICAL EXAMINATION OF
p63 SOFT TISSUE TUMORS, COMPARISON WITH RADIOLOGY?

Gielen J, De Schepper A, Vanhoenacker F. Antwerp, Belgium

11:40 CT ANGIOGRAPHY WITH VOLUME RENDERED THREE DIMENSIONAL
p65 IN PREOPERATIVE EVALUATION OF SOFT TISSUE TUMORS

Verga L, Gallo A, Martorano D, Verna V, DeMarchi A, Faletti C. Torino, Italy

11:50 SOFT TISSUE TEMPERATURE CHANGES DURING CT-GUIDED
p66 RADIOFREQUENCY ABLATION OF OSTEOID OSTEOMAS

Ludwig K, Bernd L, Rupp R, Bitsch R. Heidelberg, Germany

12:00 Lunch

VII. New Techniques, Intervention, Infection

Saturday, 13:30 – 14:50

Fuggerzimmer

Chairperson: Arkun R, Izmir, Turkey

13:30 THE POTENTIAL VALUE OF MR IMAGING IN THE SEATED POSITION:
p67 A STUDY OF 116 PATIENTS SUFFERING FROM LOW BACK PAIN AND
SCIATICA

Muthukumar T, Smith FW, Wardlaw D, Pope M. Oswestry, United Kingdom

13:40 PERCUTANEOUS VERTEBROPLASTY FOR THE TREATMENT OF
p68 OSTEOPOROTIC VERTEBRAL COMPRESSION FRACTURES AND
SPINAL COLUMN NEOPLASMS

Kupcs K, Aksiks I, Dzelzite S, Karklins E, Vestermanis V. Riga, Latvia

13:50 TRANSARTERIAL EMBOLIZATION FOR HYPERVASCULAR BONE
p69 TUMOR WITH USE OF SUPERABSORBENT POLYMER MICROSPHERES
(SAP-MS)

Nakanishi K, Osuga K, Hori S, Hamada K, Araki N, Ueda T, Yoshikawa H,
Nakamura H. Osaka, Japan

14:00 RADIOFREQUENCY ABLATION IN THE PALLIATIVE TREATMENT OF
p70 SOFT TISSUE TUMORS

Hoffmann RT, Schneider P, Reiser MF, Helmberger TK. München, Germany

14:10 MYCOBACTERIUM BOVIS BCG OSTEOMYELITIS

p71 Köllö K, Szöke G, Shisha T, Mester A. Budapest, Hungary

14:20 WHITE CELL SCAN IN PROSTHETIC JOINT INFECTIONS

p72 Munir U, Dussa CU, Herbert J. St. Helens, United Kingdom

14:30 THE VALUE OF ULTRASONOGRAPHY IN THE DIAGNOSIS OF
p73 PYOMYOSITIS

Andipa E, Bilas K, Bizimi V, Kolovou P, Liberopoulos K, Tsouroulas M, Zois G.
Greece

14:40 INFECTIOUS SPONDYLODISCITIS: (TO) BE (EARLIER) AWARE

p74 Lange C, Montauban van Swijndregt A, Van der Woude H.
Amsterdam, The Netherlands

14:40 Coffee Break

MR IMAGING IN CHANCE-TYPE FLEXION DISTRACTION (CTFD) SPINAL INJURIES

Groves, Clare, Cassar-Pullicino, Victor.

The Robert Jones and Agnes Hunt Orthopaedic and District hospital, Oswestry, U.K.

Purpose: To define the role of MRI in the diagnosis and management of Chance-type flexion distraction injury.

Methods: The clinical and imaging data of 24 patients who had sustained CTFD injuries were retrospectively reviewed. A standard proforma was utilised to record the bone and soft tissue abnormalities. The MR studies were independently reviewed by two radiologists and the findings following consensus, were correlated with the radiographs and CT appearances.

Results: At MRI, combined bony and soft tissue injuries were more common than either bone or soft tissue damage alone, and occurred at the thoracolumbar junction primarily. Contiguous vertebral injury was seen in 18 cases, with non-contiguous injury in 7 cases. Posterior ligamentous complex disruption occurred in all cases. Extensive subcutaneous and para-spinal muscle oedema was seen in all cases extending over several segments. Horizontally orientated fractures of the posterior neural arches produced a distinctive MRI pattern -"Sandwich sign"-consisting of linear haemorrhage framed by marrow oedema. Extension of the fracture into the posterior vertebral body outline occurred in 3 cases, with fracture displacement into the canal. The posterior vertebral body height remained unchanged or increased in these 3 cases.

Conclusion: The MR features of CTFD injuries are recognisable and reproducible, allowing a confident differentiation from "unstable burst injuries"

DEVELOPMENT OF A LOW DOSE MULTI-SLICE CT (MSCT) SCANNING PROTOCOL FOR USE IN SPINAL TRAUMA

C Krolak, U Linsenmaier, E Coppenrath, KJ Pfeifer, M Reiser

Purpose: Development of a low dose MSCT protocol for examination of the cervical spine in patients with spinal trauma.

Materials and Methods: The cervical spine of 3 patients (2 m, 1 f) was examined in post mortal CT (PMCT) with 3 different low-dose protocols (Somatom Volume Zoom, Siemens AG). The cervical spine examination CT protocol actually used in routine (100 mAs, 120 kV, 5mm table movement, 4 x 1 mm collimation, 2 mm slice thickness, 2 mm increment, 3 mm sagittal and coronal multiplanar reformations) was considered as gold standard. In different protocols, mAs value was changed to 100 mAs, 66 mAs, and 33 mAs. Images were subsequently analysed semiquantitatively using a quality score (ranging from 1: not evaluable to 4: excellent quality) regarding noise, discrimination of cortical and trabecular bone structures as well as artefacts. Image analysis was performed for the cranial cervical vertebral bodies (CVB) 1-4, and caudal CVB 5-7 separately.

Results: For cranial CVB image quality in the different protocols (100, 66, 33 mAs) was rated 4, 4, 4 (axial), 3, 3, 3 (coronal), and 3.5, 3.5, 2.75 (sagittal). For caudal CVB image quality was scored 3, 3, 3 (axial), 2.75, 2.75, 2.75 (coronal), and 2.25, 2.25, 2.0 (sagittal). In the low dose protocol using 33 mAs significant differences could be found in the sagittal reformation with a score of 2.75 for the cranial CVB and 2.0 for the caudal CVB, axial and coronal reformations were not significantly different from the other protocols. Highly significant differences were found with increasing noise as well as inferior discrimination of trabecular and cortical bone using 33 mAs. No significant difference could be detected for the protocols using 100 mAs and 66 mAs.

Conclusion: With increasing use of MSCT in spinal trauma low dose scanning protocols are preferable, especially in younger patients. In trauma patients, dose reduction to 33% of the gold standard protocol dose is possible with the mentioned limitations, while sufficient image quality in axial and coronar planes is obtained. Whenever the clinical question requires interpretation of sagittal reformations, dose reduction is limited to 66%.

MR Signal Alterations in the acute Onset of Heterotopic Ossification in Patients with Spinal Cord Injury

Hans Peter Ledermann, Markus F. Berger, Hans Knecht, Lukas F. Wick

Purpose: To evaluate MR-signal characteristics at the acute onset of heterotopic ossification (HO) in paralyzed patients.

Patients and Methods: 21 patients with spinal cord injury (female n=3, male n=18, mean age: 33.4 years) and acute onset of radiographically (n=12) and clinically (n=9) proven HO had 1.5T MR imaging (contrast enhanced n=17) within 11.5+-18.2 days after clinical onset of symptoms. Two musculoskeletal radiologists evaluated together MR signal alterations of affected muscles, fascia, subcutaneous tissue, skin and adjacent bone.

Results: Widespread diffuse T2-hyperintense signal of multiple muscle groups was seen in all patients (bilateral in 17 (81%)). Most involved muscles were: quadriceps (90%), adductors (75%) and iliopsoas (75%) with contrast enhancement between 50%-90% . Other MR findings included: fascial edema (n=19, 90%), fascial enhancement (n=15, 88%), subcutaneous edema (n=21, 100%), subcutaneous enhancement (n= 15, 88%), skin enhancement (n=11, 64%) bone marrow edema (n=7, 33%), joint effusion (n=15, 71%), discernible calcification or ossification (n=2, 9%). MR findings in the 9 patients with clinically proven HO were identical. Sharply defined areas without enhancement (mean size 2x3.5x5.8cm) were seen in 16/17 (94%) patients within diffusely enhancing muscles. CT correlation revealed bone formation exactly around the periphery of nonenhancing regions in three patients.

Conclusion: Acute onset of HO leads to extensive, mostly bilateral edema and enhancement of muscles, fascia, subcutaneous tissue and skin. HO occurs in severely inflamed muscles in the periphery of well-defined areas of no enhancement. Calcification or ossification is only rarely discernible on initial MR exams.

NON POST-RADIOTHERAPY PELVIC RING INSUFFICIENCY FRACTURES: DON'T MISS ASSOCIATED INJURIES.

LLOPIS E., Higuera V, Ferrer P., Muñoz I.*, Trenor P., Martínez A.

Radiology, Rheumatology and Orthopaedic Department. Hospital de la Ribera. Hospital Casa de Salud*. Valencia. Spain.

Purpose: To demonstrate that sacrum, iliac and ilii rami fractures, pelvis ring insufficiency fractures, are frequently simultaneously involved. To describe multislice CT and MRI characteristic radiological features that permits an accurate diagnosis.

Material and Methods: We have retrospectively reviewed 15 patients with multiple pelvic ring insufficiency fractures. Any of these patients had a previous history of radiation therapy. The average age was 64 years old. There were 12 women and 3 men. The MRI study was performed in a 1T unit, with SE T1 and STIR sequence in axial and coronal planes in the pelvis and oblique coronal for the sacroiliac joint, multislice CT was performed in 12 patients with posterior multiplanar reconstructions, MPR and curved-MPR.

Results: All patients presented multiples fractures, 13 patients had sacrum fractures (11 bilateral), 12 patients ileopubic rami (7 bilateral), 9 patients isquiopubic rami fractures and 2 patients supracetabular fractures. Two patients with sacrum fractures showed obturator muscle oedema without pubic rami fracture. All sacrum fractures showed characteristic hypointense band in T1W and marrow oedema in STIR sequence parallel to the sacroiliac joint, 4 of them had also transverse band through the sacrum vertebra (H-shaped pattern). Aggressive aspect of fractures of the pubic rami (iliac and ilii) was showed in 9 patients. The typical fluid collection within the fracture gap was seen in 8 patients.

Conclusion: Characteristics imaging findings and location permit an accurate diagnosis of insufficiency fractures and can avoid inappropriate studies and bone biopsies. SE T1 and T2-fat suppression or STIR sequences are the more adequate sequences to define the fracture line, marrow and soft tissue oedema. Curved multiplanar reconstructions are the more useful reformatted images for sacrum imaging. The aggressive aspect of pubic rami fractures is produced by distraction of the fragments and muscle oedema, a cleft like fluid collection aids for the diagnosis. Usually characteristic MRI aspect of sacral fractures allows the radiological diagnosis. Multislice CT must be limited for inconclusive cases in an attempt to demonstrate the fracture line. Due to abnormal stress across the pelvic ring a fracture in a segment can lead to secondary abnormalities, fracture or muscle sprain, so a complete MRI study must be performed to despite occult injuries.

Avascular osteonecrosis of the proximal fragment in scaphoid nonunion: Is intravenous application of contrast agent really necessary ?

R. Schmitt, G. Coblenz, S. Fröhner, K. Megele, H. Krimmer, G. Christopoulos
Bad Neustadt/Saale (D)

Purpose: Unenhanced MRI displays the osseous viability by means of the high signal intensity of normal fatty marrow in T1-w images as well as by demonstrating bone marrow edema which is hyperintense in all fat-suppressed T2-w sequences. The aim of our study was to assess the diagnostic value of intravenously applied contrast agent for the diagnosis of osteonecrosis of the proximal fragment in scaphoid nonunion, and to compare the imaging results with intraoperative findings.

Material and Methods: 88 patients (7 women, 81 men, age 16 to 52 years) suffering from symptomatic scaphoid nonunion were included in a prospective study. Preoperatively, MRI was performed with the following sequences: coronal PD-w FSE fat-suppressed, sagittal-oblique T1-w SE plain, sagittal-oblique contrast-enhanced T1-w SE fat-suppressed, sagittal T2*-w GRE (MEDIC). MRI interpretation was based on the intensity of contrast enhancement: 0 = no enhancement, 1 = focal enhancement, 2 = diffuse enhancement. Intraoperatively, the osseous viability was judged by assessing punctate bleeding points on the osteotomy site of the proximal scaphoid fragment. The intensity of bleeding points were scored: 0 = missing, 1 = moderate, 2 = good. Results underwent statistical analysis.

Results: The hand surgeons found 17 complete osteonecroses, 29 compromised, and 42 healthy proximal fragments. In unenhanced MRI bone viability was judged as follows: complete necrosis in only 1 patient, compromised in 20 patients, and unaffected in 67 patients. Contrast-enhanced MRI revealed different findings: complete necroses in 14 patients, compromised viability in 21 patients, and normal bone marrow in 53 patients. Judging surgical findings as the standard of reference, statistical analysis led to this assessment for unenhanced MRI: sensitivity 6,3%, specificity 100%, positive PV 100%, negative PV 82,6%, and accuracy 82,9%, and for contrast-enhanced MRI: sensitivity 76,5%, specificity 98,6%, positive PV 92,9%, negative PV 94,6%, and accuracy 94,3%. Most obvious was the very low sensitivity ($p < 0,001$) revealing insufficient detection of avascular osteonecrosis by using unenhanced MRI.

Conclusion: It was clearly demonstrated that the presence of bone marrow edema doesn't rule out osteonecrosis in the proximal fragment of scaphoid nonunion. According to our findings viability is more accurately assessed by means of signal behavior in contrast-enhanced MRI. We strongly recommend the application of intravenous contrast agent for the imaging of the scaphoid nonunion.

COMPARISON BETWEEN 16 DETECTOR MULTISLICE CT AND SKELETAL SCINTIGRAPHY IN THE DIAGNOSIS OF OCCULT SCAPHOID FRACTURES: DISCRIMINATIVE VALUE OF QUANTIFICATION OF ^{99m}Tc-MDP UPTAKE

A M Groves, H K Cheow, P W P Bearcroft, M Coleman, H Wood, K K Balan, A K Dixon

Purpose To compare the measured uptake of ^{99m}Tc-methylene diphosphonate (^{99m}Tc-MDP) in those scaphoid fractures seen on both 16 detector multislice CT and scintigraphy, with those seen only on scintigraphy

Materials and methods Over a 12 month period a total of 51 patients with suspected fracture underwent both conventional ^{99m}Tc-MDP scintigraphy and 16 detector multislice CT. A total of 23 fractures were identified on scintigraphy of which 16 were also detected on CT (concordant). In 7 cases the fracture was not seen on CT, even in retrospect (discordant). In the discordant cases, follow-up radiographs and MRI (where available) also failed to demonstrate a fracture.

The ^{99m}Tc-MDP uptake was measured by placing a region of interest (ROI) over the fracture site and the mean and maximum number of counts were compared to those in a similar size ROI placed over background bone activity.

Results The mean fracture count to background bone activity ratio averaged 7.7 (range 3.2 to 18.5) for concordant fractures and 3.8 (range 1.7 to 5.3) for discordant fractures (t-test P=0.04).

The maximum fracture count to background bone activity ratio averaged 12.7 (range 4.3 to 27.7) for concordant fractures and 6.3 (range 2.6 to 9.5) for discordant fractures (t-test P=0.03).

Conclusion The ^{99m}Tc-MDP uptake was significantly higher in concordant fractures than in discordant fractures. The authors speculate whether these discordant fractures with less ^{99m}Tc-MDP uptake may represent a less severe injury, such as bone bruise rather than cortical fracture.

FRACTURES OF THE TOP OF THE GREATER TROCHANTER AT RADIOGRAPHY AND ITS ASSOCIATION TO AN INTRA-TROCHANTERIC FRACTURE AS DEMONSTRATED BY MR IMAGING: DISCUSSION OF CLINICAL AND SURGICAL CONSEQUENCES

Gelineck J¹, Andersen K², Egund N¹

Department of Radiology R¹ and Orthopaedic Surgery E²

Aarhus University Hospital, 8000 Aarhus C, Denmark

Purpose: To present at MR imaging the course and extension of occult intertrochanteric fractures associated with “avulsion” fractures of the top of the greater trochanter and discuss their clinical and surgical significance.

Patients and methods: A displaced pertrochanteric fracture was registered 5 days after trauma with an isolated “avulsion” of the greater trochanter at radiography in 2000. Since then, an increasing number of patients with these “avulsions” had obtained MR imaging and osteosynthesis. Four males and 15 females aged 44 to 90 years (mean 77 years), right/left, 9/10. The time between the radiographic examination and the MR imaging ranged between 1 and 335 hours (mean 59 hours). The routine MR sequences were in all patients oblique coronal STIR and T1. Six patients also obtained oblique coronal T2 and 6 patients either transaxial STIR or T1.

Results: The vertical length at radiography of the “avulsion” of the greater trochanter varied between 10 and 45 millimetres. Displacement of the fragment was seen in 7/19. At T1 weighted MR imaging sequences all patients except one demonstrated a circular fracture line surrounding the greater trochanter with an extension in the distal direction of 40-80 mm (4.9 mm). In 9/18 hips it was assessed that the vertical fracture had additional fractures extending to the medial cortex of the femur. The T1 weighted sequence only demonstrated the course of the fracture in all patients. 14/18 patients obtained nailing.

Discussion and conclusion: Almost all patients with “avulsion” of the greater trochanter had occult fractures of the proximal femur, but not with the usual course of a pertrochanteric fracture. It is felt that the group of elderly patients with hip trauma and “avulsion” of the greater trochanter represents the tip of the iceberg of occult fractures of the hip and that MR imaging may result in unnecessary surgical interventions. Recognition of the fracture and its occurrence also in patients without the “avulsion” at future scientific MR studies may be helpful for the mobilization process of the patients with hip trauma and negative radiographs.

Reference

Graig JG et al. Fractures of the greater trochanter: intertrochanteric extension shown by MR imaging. *Skeletal Radiol* (2000) 29:572-576

EVALUATION OF ORGAN DOSES AND EFFECTIVE DOSE FOR PELVIC AND LUMBAR SPINE EXAMINATIONS USING A C-ARM BASED CT-SYSTEM IN COMPARISON TO A SINGLE SLICE CT

Fischer T, Linsenmaier U, Kotsianos D, Wirth S, Goldbrunner H, Pfeifer KJ, Reiser M

Department of Clinical Radiology, Ludwig-Maximilians-University, Munich

Purpose: Calculation of organ doses and effective dose for examinations of the pelvis and lumbar spine with a new mobile C-arm based 3D CT system in comparison to spiral CT.

Materials and Methods: The ISO-C-3D (Siemens Medical Solutions, Erlangen) is a mobile C-arm image amplifier with a 3D CT option. Multiplanar high contrast cross-sectional images with a 10cm FOV can be reconstructed out of a data cube that is generated from 100 projection images acquired during a single 190° rotation of the isocentric C-arm. Examinations of the pelvis and lumbar spine were performed with ISO-C-3D and spiral CT (Siemens Somatom Plus 4) using an Alderson phantom containing 30 TLDs (thermo luminescence dosimeters) positioned at different organ levels (e.g. ovary, bone marrow, breast). The ISO-C-3D scans were executed in an automatic exposure mode (80-95kV) with a predetermined slice thickness (SL) of 0,46mm. For comparison with the spiral CT, standard protocols were used (120kV,200mAs, SL 3mm/pitch 1.5). After radiation exposure of the TLDs the organ doses were evaluated, out of which the effective doses could be estimated.

Results: Pelvic studies yielded the following organ doses (in mGy): bone marrow (ISO-C-3D:1.4/ spiral CT:1.2); ovary(7/6); colon(3.3/2.9); stomach(0.1/0.1); bladder(10/7); breast(0.1/0). Lumbar spine studies showed the following doses (in mGy): bone marrow(ISO-C-3D:2.2/ spiral CT:2.2); ovary(3/1); colon(7.3/5.8); stomach(4.3/1.2); bladder(0.5/0.2); breast(0.1/0.5). The resulting effective doses (ISO-C-3D/CT) were 2.6mSv/2.15mSv for pelvic scans and 2.73mSv/2.23mSv for lumbar spine examinations.

Conclusion: Organ doses and effective doses are slightly higher for ISO-C-3D scans compared to spiral CT scans. Therefore using the ISO-C-3D during operations for controlling the bone position, the number of conducted scans should be kept as low as possible. Due to the exposure data and the limited image quality the use of ISO-C-3D is not recommended for diagnostic purposes.

Multidetector row CT versus digital radiography in the evaluation of bone healing in orthopedic patients

Krestan C.R., ¹Noske H., Vasilevska E, Schuller G, Czerny C., Imhof H

Department of Radiology, Division of Osteoradiology

¹Department of Orthopedic Surgery

Medical University of Vienna

Purpose:

Bone healing or failure to do so in orthopedic patients is usually monitored by radiographs in two views. The purpose of our study was to compare the efficiency of multiplanar reconstructions (MPR's) of multidetector row CT (MDCT) datasets to digital radiographs in assessing the extent of bone healing.

Materials and Methods:

47 orthopedic patients (19 female, 28 male) after arthrodesis, fractures or spinal fusions who underwent a MDCT exam and radiographs were included into our study.

MDCT studies were performed on a MX 8000IDT (Philips Medical Systems, Best, The Netherlands) and served as the gold standard. The technical parameters were as follows: 16 x 1.5 mm collimation, slice thickness 2mm, RI 1mm, 150 mAS, 140 kV, bone window (3500/600 HU). Multiplanar reconstructions (3mm/3mm) were calculated from the axial slices in two orthogonal planes. All patients underwent digital radiographs on a Multix FD system (Siemens Medical Solution, Erlangen, Germany) in two views according to standard procedures.

MPR's and radiographs were analysed by two musculoskeletal radiologists as a consensus reading with regard to bone healing using a semiquantitative approach (complete, partial, non-union).

Results:

In 24(51%) patients there was agreement between MDCT and radiography with respect to the extent of bone healing, whereas in 23 (49%) patients the results were not concordant.

In 12 patients (25.5%) digital radiographs underestimated the extent of bone healing, whereas in 11 patients (23.5%) overestimation of the degree of fusion was observed. In the case of 11 (23.5%) patients with metal implants, artefacts did not affect the assessment of bone fusion significantly.

Conclusion:

MDCT with MPR's is superior to digital radiography in the evaluation of bone healing and should be the preferred diagnostic modality.

ACCURACY OF COMPUTER-ASSISTED PIN PLACEMENT USING A FLUOROSCOPY GUIDED NAVIGATION SYSTEM AND A NOVEL TARGETING DEVICE: A PHANTOM STUDY

RJ Bale, P Kovacs, T Lang, M Knoflach, RE Rosenberger, C Hoser, M Blauth, W Jaschke

Purpose: To determine the accuracy of computer-assisted targeting using a novel fluoroscopy guided navigation system in combination with a novel targeting device in a phantom study as a prestudy for application in emergency surgery.

Materials and Methods: A phantom was built with stepwise arrangement (3 steps) of two different materials and screws (n=60) serving as target points. Four fluoroscopic images were acquired from different directions and sent to the FluoroNav navigation system (Medtronic Inc., USA). The tips of the screws were identified on the c-arm images and for every target a drilling path was planned with the navigation system. Pins with two different diameters (1.0 and 2.5mm) were advanced to the targets using the Vertek targeting device which was developed by our group in collaboration with Medtronic/USA and Medical Intelligence/Germany. Using the pin with 2.5mm diameter every target was localized 10 times (n=60). 1.0 mm pins were advanced into the lower two steps (n=40). The accuracy of pin placement was evaluated using CT (1.25mm slice thickness).

Results: The mean localization error for all drillings was 2.3 ± 0.9 mm (range: 0.4 to 6.4mm). The errors were higher in the polystyrene material in comparison to the aerated concrete. 1.0mm pins were less accurate than 2.5mm pins. In addition, error increased with the length of the pathway.

Conclusions: The results of the phantom study indicate that computer-assisted fluoroscopy guided drillings in combination with a novel targeting device allows for accurate localization of different targets. The diameter of the pin has to be selected according to the depth and the tissue on the way to the target.

ULTRASOUND EVALUATION OF PECTORAL MUSCLE INJURIES

A Rehman, P Robinson.

Leeds Teaching Hospitals, Leeds, United Kingdom.

PURPOSE: To demonstrate the application of high resolution ultrasound for the diagnosis and grading of pectoral muscle injuries.

MATERIALS AND METHODS: A retrospective analysis of five consecutive cases (4 male, 1 female, age range 26-45) referred for assessment of a pectoral girdle injury. Three cases presented following a fall involving a combination of forced abduction, external rotation and extension while two cases presented after lifting heavy objects. Ultrasound examination of the chest wall and arm was performed by a musculoskeletal radiologist using a high frequency linear transducer. The three heads of pectoralis major as well as pectoralis minor, biceps, deltoid and rotator cuff were assessed in the long and short axis of the muscle and tendon both at rest and dynamically. Injuries were prospectively graded 1- 3 according to a recognised classification system as; partial tear of the myotendinous unit with less than 5% of the muscle involved (grade 1), greater than 5% involved (grade 2) and a complete full thickness tear (grade 3). If detected the location of the pectoral muscle tear was recorded as origin, peripheral, myotendinous junction or enthesis. The clinical course of all cases was followed by case note review at 6 weeks, 3 months and 6 months.

RESULTS: 4 cases had injuries of pectoralis major and one case had an injury to pectoralis minor. Three cases had complete (grade 3) tears of the sternal head at the myotendinous junction with two of these three cases having further grade 3 injuries of the abdominal components and high grade injury to the clavicular components (one grade 2 and one grade 3). The fourth case was found to have a grade 2 myotendinous junction tear of pectoralis minor. The fifth case had a grade 2 tear at the origin of the sternal head. Therefore four (80%) injuries were at the myotendinous junction, one (20%) was at the proximal sternal origin and none were identified at the enthesis.

CONCLUSION: Pectoralis major injury is an uncommon injury but differentiation of complete and partial tears is imperative in orthopaedic surgical management planning. The myotendinous junction and distal tendon have a complex anatomy which can make visualisation in standard MR imaging planes difficult. Ultrasound provides rapid multiplanar dynamic assessment of this region and is not degraded by local oedema as can occur with MR imaging.

Knee joint 3D model reconstructed with CT and MRI images: an innovative concept for biomechanical study of bone and soft structures

Ramaniraka NA, Siegrist O, Terrier A, Theumann N

Centre de Recherche en Orthopédie, EPFL, CH Hôpital Orthopédique de la Suisse Romande, Lausanne CH Service de Radiologie, CHUV, Lausanne, CH

OBJECTIVE: The goal of this study was to develop an anatomic 3D finite element model for biomechanical study of a knee joint including bones (femur, tibia, patella, fibula) and soft tissue (ligaments, tendons, cartilage and menisci) in order to study the physiological, pathological and post-surgical biomechanics.

METHODS: MR imaging (spin echo T1-weighted sequences in sagittal, coronal, axial and oblique coronal planes) and CT-scanner (1.2mm, pitch 1) of the right knee of one healthy volunteer were performed. Superimposing MRI planes and then segmentation of the soft structures with Amira software were performed. 3D reconstruction of bone geometry was realized with CT data. Geometric 3D anatomical model was then obtained by matching segmented soft structures and 3D model of bone from CT images. Digitalized modeling in finite elements was realized. With this model, the muscle forces (semimembranosus and biceps femoris for flexion, quadriceps femoris for extension) could be simulated to get 90 degrees of flexion and full extension of the knee joint. Pressure at the tibio-femoral and menisco-femoral contact interfaces and stress inside the posterior cruciate ligament (PCL) were calculated with the standard model, after PCL removal and after PCL reconstruction (synthetic and autograft stiffness taken from the literature).

RESULTS: First, with the standard model, the pressure in internal (IFT) and external (EFT) femoro-tibial compartment were comparable with human measures in the literature. After PCL removal, EFT pressure remained equal but IFT pressure increased (50%). PCL synthetic graft reconstruction produced an increase of pressure at the tibio -femoral interface (30%) and increase stress inside the graft (400%).

CONCLUSIONS: Testing of the model confirmed clinical situations, for instance IFT osteoarthritis after PCL rupture, or synthetic graft rupture due to the increased pressure inside the graft. The technological association of radiologist, orthopedist and engineer showed to be necessary for realizing an advanced model to study the knee joint biomechanics. Further simulations are in progress.

QUANTITATIVE COMPUTED TOMOGRAPHY IN THE EVALUATION OF BONE DENSITY IN

G. ALZEN, D. Berthold, D. Moritz.

Kinderradiologie, Justus Liebig Universität Giessen, Germany.

Purpose: To establish a quantitative computed tomography osteodensitometry protocol in pediatric patients measuring spongy bone density in only one lumbar vertebra and to determine normal values and a threshold for spontaneous vertebral fracture.

Materials and Methods: In a prospective study we performed 110 osteodensitometry tests in 94 patients (mean age 13 years, range 2 months to 23 years). 36 patients with normal bone mineral density consented to the test while being investigated by CT for non-related reasons. 58 patients had suspected bone mineral loss.

Results: The average trabecular bone density in healthy individuals was equivalent to 157 mg Ca-hydroxyapatite (HA) per ml bone with a difference between boys (147 mg Ca-HA/ml) and girls (165 mg Ca-HA/ml). There was an increase during the first and second decade; the density in early adolescence was lower than of young adult patients. Patients with fractures were below 70 mg/ml Ca-hydroxyapatite with one exception, where there was compression of the vertebral bodies.

Discussion: In healthy patients, bone mineral density was lowest in pre-pubertal children. During the late adolescence density values increase. Fractures of vertebral bodies occur below a trabecular bone density of about 70 mg Ca-HA/ml.

IDENTIFICATION OF OSTEOPOROTIC VERTEBRAL FRACTURES IN POSTMENOPAUSAL FEMALES ON LATERAL CHEST RADIOGRAPHS

M Calleja, I Chasi, G Hide

Purpose: To determine the sensitivity of radiological reports for thoracic vertebral fractures on lateral chest radiographs in a group of elderly females, and to assess the effect of the report on further patient management.

Materials and Methods: Lateral chest radiographs performed on a group of post-menopausal women during the period April 2001 - March 2002 were reviewed. Radiographs were independently assessed by two radiologists for the adequacy of demonstration of the individual vertebrae and for the presence of fractures. Fractures were graded using an accepted semiquantitative analysis method. Correlation was made with the original radiology report, and the patients' medical notes were scrutinised for evidence of recognition and treatment of osteoporotic fractures.

Results: Radiographs were reviewed for 277 patients having a mean age of 73.8years. There was good correlation between the two assessing radiologists (Kappa 0.776, 89.9% agreement for all fracture grades). Eighty patients had fractures. In only 16 cases (20%) were these mentioned in the radiology report. Of these patients, 7 were not on any osteoporosis treatment and the remaining 9 were being treated appropriately. Seven patients whose fractures were not mentioned in the x-ray report were on osteoporosis treatment, either co-incidentally or because their clinician had identified the fracture. Fifty seven patients, (71.4% of all cases with fractures) whose fractures were not mentioned in the report, were not on appropriate osteoporosis treatment.

Conclusion: Detection of osteoporotic vertebral fractures in postmenopausal women by radiologists and clinicians was poor, suggesting that some women who should be considered for osteoporosis treatment are not being identified.

Diagnosis of Osteoporosis: Visual assessment of conventional und digital radiography in comparison with dual X-ray absorptiometry of the lumbar spine

A Baur-Melnyk, A Stähler, H Sittek, H Bonel, G Laeverenz, M Reiser

Purpose: To analyse the visual detection of osteopenia of digital in comparison to conventional radiographs.

Patients and Methods: We retrospectively evaluated the x-rays of the lumbar spine of 286 patients without vertebral fractures. 158 patients had digital, 128 patients conventional radiographs. 4 experienced and independent musculoskeletal radiologists assessed, blinded to the values of DEXA, if the bone density of the lumbar spines were normal or osteopenic/osteoporotic. The results of dual X-ray absorptiometry (DEXA) of the lumbar spine served as gold-standard. Treshold value for the diagnosis of osteopenia/osteoporosis was a T-Score less than -1 SD/ $-2,5$.

Results: Diagnostic accuracy was 68% for conventional and 64% for digital radiographs, respectively. Sensitivity/Specificity was 86%/36% for conventional and 72%/47% for digital radiographs. 80% of patients with osteopenia ($T < -1$ and $> -2,5$) and 96% of patients with osteoporosis ($T < -2,5$) were correctly assessed as true positive on conventional and in 65% (osteopenia) and 82% (osteoporosis) on digital radiographs. Interobserver agreement was significantly lower for digital radiographs (35,4%) than for conventional radiographs (73,4%).

Conclusion: Detection of osteopenia /osteoporosis is still very difficult to assess visually. There is no significant difference for digital versus conventional radiographs.

Vertebral assessment by plain X-rays film: accuracy and precision of an automatic software

G Guglielmi¹, A Brett², J Haslam², K Walker², MG Placentino¹, F Catalano³

¹Department of Radiology, Hospital “CSS” San Giovanni Rotondo, Italy

²Image Metrics PLC, Regent House, Heaton Lane, Stockport SK4 1BS, UK.

³Procter & Gamble Pharmaceuticals, Rome, Italy

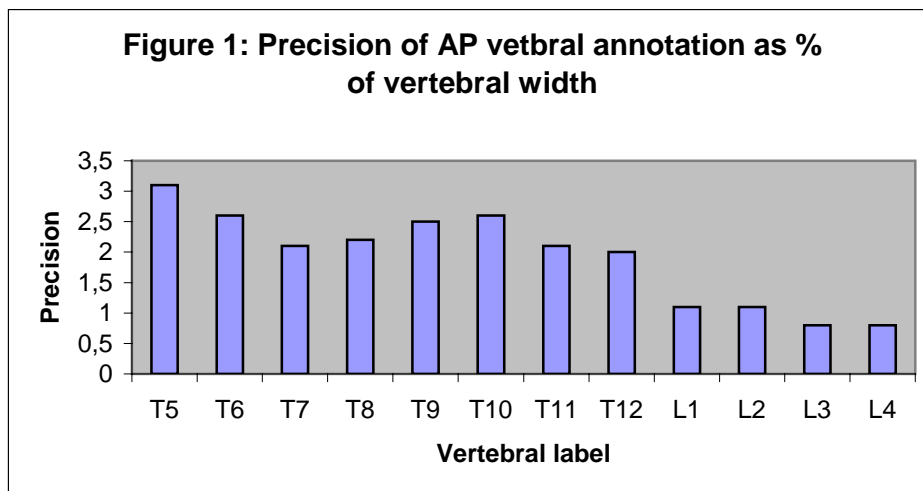
Purpose: To determine the accuracy and precision of a software application based on statistical modelling (*MorphoXpress*) for the automated placement of landmarks for 6-point vertebral morphometry from digitised plain X-rays film.

Materials and Methods: A sample of 92 lateral vertebral assessment plain film X-rays images (half analogical and half digital, normal, under and over exposed films) indicating both normal anatomy and vertebral fractures were digitised and analysed. Automated analysis was initialised by the manual labelling of the centres of the upper and lower vertebrae to be landmarked. After automated landmarking, a well trained musculoskeletal radiologist manually moved any inaccurately positioned points before confirmation of the result. Accuracy was calculated for individual vertebrae as mean rms errors between automated point positions and confirmed manually corrected positions. Precision was assessed on 20 of the images and corresponding simulated user input data computed from manual annotation. Simulated user input data was varied by adding an offset calculated in both x and y from a random Gaussian distribution of SD = 2.5% vertebral width. Each image was landmarked in this way 10 times and the mean rms error calculated. In both experiments, errors were determined as Anterior-Posterior (AP) or Superior-Inferior (SI) in the frame-of-references of individual vertebra. Vertebrae with errors >3 SD from the mean rms error were discounted as failures of automated landmarking. Due to variability in resolution of digitisation and lack of calibration data, all AP and SI errors were normalised as fractions of individual vertebral widths.

Results: Cumulative distribution of accuracy errors gave a threshold of ~2.5% vertebral width, below which no manual correction of points by radiologist were made. Accuracy results are presented in Table 1 and precision results are presented in Table 2. No vertebrae were discounted as failures of landmarking in the precision test. Figure 1 shows how AP precision depends upon vertebral label.

TABLE 1
Accuracy of semi-automated 6-point assessment measured in the frame of reference of local vertebral level, errors are normalised by local vertebral widths.

Vertebral Level	AP Error %	SI Error %	Vertebrae Analysed	Number of Failures
T5	1.4	1.5	12	5
T6	2.8	2.4	17	5
T7	3.9	3.2	17	4
T8	2.6	2.1	19	5
T9	3.5	2.5	19	6
T10	2.5	2.0	21	8
T11	2.9	2.3	28	4
T12	2.1	2.0	53	3
L1	2.5	2.5	76	3
L2	2.2	2.3	73	4
L3	2.0	1.7	70	2
L4	1.6	1.5	61	4



Conclusion: The majority of failures of landmarking in the accuracy test can be attributed to a small number to poor quality images for which multiple vertebrae were discounted. The greater accuracy and precision in the L1-L4 region may be attributed to less visual clutter in the image from overlying structures such as the ribs. The automatic application tested in this study represents a further advance towards the automation of vertebral morphometry.

The influence of posterior instrumentation on adjacent and transfixed facet joints in patients with thoracolumbar spinal injuries: a morphological in vivo study using computed tomography osteoabsorptiometry.

S Wagner, MD*, M Müller-Gerbl+, MD, A Weckbach, MD°

*Institute of Clinical Radiology, Ludwig-Maximilians-University Munich, Germany +Institute of Anatomy, Ludwig-Maximilians-University Munich, Germany °Department of Trauma and Reconstructive Surgery, University Hospital Würzburg, Germany

Purpose. To examine the influence of posterior instrumentation on content and distribution of subchondral mineralization as a correlate of the long-term load acting on the adjacent and transfixed zygapophyseal joints.

Materials and Methods. 23 patients with vertebral body fractures of the thoracolumbar junction were evaluated. After CT-scanning (5122 matrix, slice thickness 3 mm) within routine diagnostics they received bisegmental posterior fixation with an internal fixator which was removed 9.4 (* 2.5) months later. Patients were divided into two groups according to the delay between implant removal and second CT-scans: group A: 15 patients, follow-up CT-scans within less than 3 months after implant removal (average 7.3 days), group B: 8 patients, follow-up CT-scans 6 and more months (average 17 months) after implant removal. The subchondral bone plate of the zygapophyseal joint facets was isolated and reconstructed in 3D. For every image point the maximum HU value of the underlying subchondral bone was projected onto the reconstructed joint surface. Hounsfield values were summed up by steps of 100 units and encoded as false color map. For quantitative analysis the number of pixels per HU unit was calculated and every HU value was given a calcium value by reference to a phantom with known calcium concentration. The subchondral mineralization content in milligrams of calcium per milliliter was then calculated for the whole joint surface by integration of the HU distribution graph and taking account of the surface size of the joint. HU maps and mineral density distribution graphs were compared to evaluate intraindividual changes in mineralization pattern and content of paired facet joints.

Results. There was a significant difference between pre- and postoperative calcium values (p-value < 0.001, Wilcoxon test) for the total sample of patients. Mineralization decrease was more often found than increase (p-value < 0.001, Wilcoxon test). In group A an overall mineralization decrease was found in contrast to an overall mineralization increase in group B (p-value < 0.001, Mann-Whitney test). In group A a mineralization decrease was shown in 61.3 % and an increase in 11.0% of the facet joints, whereas in group B a mineralization decrease was found in 21.9% and an increase in 41.0%. There were no significant differences between adjacent and transfixed facets in group A (p-value = 0.156, Kruskal-Wallis test). However, in group B the suprajacent joints showed a higher mineralization increase than the transfixed joints (p-value = 0.030, Wilcoxon test).

Conclusion. Decrease of subchondral mineralization in patients with early follow-up CT-scans indicates reduced load acting upon the examined zygapophyseal joints and may be caused by reduced patient mobility and activity until implant removal. Increase in subchondral mineralization in patients with longer delay between implant removal and second CT-scans is considered to reflect higher load acting on both adjacent and bridged joints which is likely to be caused by the unphysiological long-term stress induced by posterior stabilization. Whether or not this disproportion of load-bearing capacity due to demineralization and increased external stress due to stabilization leads to spondylarthritis has to be studied in a long-term follow-up.

Harris Lines of the Tibia across Centuries: A Comparison of Two Populations, Medieval and Contemporary in Central Europe

S. Ameen¹, L. Staub², F. Ballmer³, S. Ulrich², P. Vock¹, S.E. Anderson¹

1 Department of Diagnostic Radiology, University Hospital of Bern, Inselspital, CH-3010 Bern, Switzerland

2 Institute of Historical Medicine; University of Bern, CH-3012, Switzerland

3 Department of Orthopaedics, University Hospital of Bern, Inselspital, CH-3010 Bern, Switzerland

Objective:

1. To determine the incidence of Harris stress lines in a contemporary population in central Switzerland and to compare the results with those in a medieval population who inhabited the same geographical area.
2. To describe a simplified method to determine the age of individual at the time of formation of Harris lines in the distal part of the tibia.

Design and patients: Radiographs of 112 well preserved tibiae of skeletons from the eighth to thirteenth century were reviewed for the presence of Harris lines. They were compared with the findings in radiographs of 148 current patients living in the same geographic location. The incidence of Harris lines were estimated in both populations, and the age of the bone at the time of their formation were estimated according to the tables of Maat.

Results: Harris lines were found in 88/112 (80%) of the examined medieval skeletons and in 20/148 (20%) of the living individuals. The peak incidence of Harris lines occurred between the age of 1-14 years in both populations. Harris lines in the contemporary populations accompanied other diseases like; osteoarthritis, peripheral vascular diseases, rheumatoid arthritis, rickets and deformities of the lower limb.

Conclusion:

1. It is very interesting to find out that there are causes other than nutritional to be associated with the appearance of Harris lines, as a reaction of the bone to a stressful condition.
2. Measuring the age of the individual at the time of formation of Harris lines may have future application in the medicolegal purposes and also in metabolic bone setting like osteoporosis

STUDY TO DESCRIBE THE MORPHOLOGY OF A SERIES OF CLAVICLES & THE DIMENSIONS OF ITS INTRAMEDULLARY CANAL.

M Ahmad, MJ Trehwella, NC Bayliss

University Hospital of North Tees, Stockton, United Kingdom

AIM:

A study was done to investigate the range in size and morphological features of a series of human clavicles.

METHOD:

A Phillips CT scanner was used to examine morphometric properties of 42 right and 36 left adult cadaveric clavicles. The resulting data was analysed with Voxar 3D software. The length of the s-shaped clavicle was measured and the planar cross-sectional geometry of the intramedullary canal and cortical thickness assessed at 10% increments along the length of the bone. MPR (multi-plane reformat) imaging allowed 'fly-through' reconstruction of cross-sectional morphology as one travels along the length of the bone.

RESULTS:

The sample studied followed a normal distribution with mean size= 136.2mm (range: 112.6-172.0 mm). In general the sternal portion of the clavicle is circular or prismatic in cross-section where as the acromial portion is flatter on its superior and inferior surfaces. A spacious, variably shaped canal is observed at the sternal and acromial thirds in contrast to the denser, smaller, more circular shaped canal in the central third of the bone. Unlike most long bones, the clavicle was observed to have an extensive network of trabeculae along the entire length of the intramedullary canal. The central third of the clavicle has the thickest cortex. The mean cortical thickness (3.37mm; range: 1.8- 7.9mm) was greatest at a point 60% from the sternal end with the mean thinnest cortex (1.37 & 1.15mm) found at the extreme sternal and acromial ends of the bone respectively.

CONCLUSION:

The clavicle is highly variable in shape and exhibits dramatic variations in both curvature and cross-sectional geometry along its length. Contrary to previous teaching, MPR reconstruction accurately demonstrates clear visualization of a distinct intra-medullary canal.

ULTRASOUND ASSESSMENT OF EARLY CLUBFOOT TREATMENT

Y Aurell¹, H Andriessse², A Johansson³ and K Jonsson⁴

¹Department of Diagn.Radiology, Halmstad County Hospital, S-301 85 Halmstad, Sweden

²Department of Orthopaedics, Lund University Hospital, S-221 85 Lund, Sweden

³Department of Orthopaedics, Skövde County Hospital, S-541 85 Skövde, Sweden

⁴Department of Diagn.Radiology, Lund University Hospital, S-221 85 Lund, Sweden

Purpose: To sonographically assess the early anatomical outcome in two differently treated groups of children with clubfeet and relate the sonographic findings to the clinical evaluation and the chosen surgical procedure and operative findings.

Material and Methods: We prospectively followed the very early clubfoot treatment in 28 clubfeet in 21 infants from the neonatal period to the age of 5-15 months by using 3 easily defined and reproducible US projections. Nine of the feet were treated by the Ponseti method (Group A) with serial castings and achillotenotomi and 19 according to a modified Copenhagen protocol (Group B) with a flexible plexidur splint and more extensive surgery. Ultrasound (US) investigations were made at three times: in the neonatal period, after 2-3 months of non-surgical treatment and 1-2 months after the first surgical event. A control group of 50 healthy age-matched babies was used for comparison.

Results: By US the talo-navicular and the calcaneo-cuboid relationship were described, quantified and compared to a control group of children with normal feet. The clinical severity of the clubfoot deformity was assessed parallel to the US investigations using the Diméglio scoring system. The distance between the medial malleolus and the navicular (the MM-N-distance) was significantly shorter in the clubfeet than in the control group. After two months of non-surgical treatment the correction obtained at the talo-navicular joint was significantly greater in the group of feet treated by the Ponseti method than in the Group B feet. Before treatment the clubfeet in both groups showed a tendency to medial displacement of the cuboid. After surgery (achillotenotomi for all Group A feet and posterior release or posteromedial release for 13 of the Group B feet) the anatomical correction at the talo-navicular and calcaneo-cuboid joints, as assessed by US, was similar for the two groups. The measurements showed an acceptable intra-and inter-observer reliability.

Conclusion: With US it is possible to assess the severity of the deformity of the talo-navicular and the calcaneo-cuboid joints and the effects of treatment can be followed quantitatively. Anatomical correction of the displacement in these joints can be achieved without extensive interventional procedures.

Complete and incomplete finger pulley disruption: HR-US evaluation in a cadaver model

Gerd Bodner, Maria Bernathova, Max Rasp, Peter Kovacs, Florian Kamelger, Markus Gabl

Purpose: to assess whether high resolution ultrasound (HR-US) allows to differentiate between complete and incomplete pulley disruption in a cadaveric finger model.

Material and Methods: 48 fingers of 12 cadaveric hands were examined by means of HR-US. After soft tissue resection and preparation of the flexor tendon and the annular pulleys A1, A2, and A3, partial and complete disruption of the A2 and combined complete disruption of A3 was performed. Fingers were fixed in a flexed position (10 ° at the distal interphalangeal-joint 40° at the proximal interphalangeal-joint) 15 kg were attached at the musculo-tendineous junction of the flexor muscles. HR-US was performed in a longitudinal scan and measurements were taken at the mid-part of the proximal phalanx between the bone and the volar side of the flexor tendons.

Results: The distance between bone and tendon was significantly higher in complete dissection of A2 than in partial disruption of A2. A significant further increase of bow stringing was seen in complete A2 - A3 disruption.

Conclusion: HR-US reliably distinguish incomplete from complete A2 pulley disruption and combined A2, A3 pulley disruption in a cadaveric model.

SYMPTOMATIC PROXIMAL PATELLAR TENDINOSIS : CORRELATION BETWEEN POWER DOPPLER ULTRASONOGRAPHY (PDU) AND CLINICAL SEVERITY

Brys P, Geusens E, Van Breuseghem I, Van Cleynenbreugel J, Peers K, Bellemans J

Purpose

This study evaluates correlations between clinical severity and findings on ultrasonography, including quantification of neovascularisation on PDU in symptomatic proximal patellar tendinosis.

Materials-Methods

73 sporters with a painful proximal patellar tendinopathy and ultrasonographically established tendinosis, excluding previous surgery or ESWT, were evaluated. After gray-scale-US examination, neovascularisation was quantified on sagittal PDU-images (5-12MHz, PRF 1000Hz, HDI 5000 ATL-Philips Ultrasound) using surface measurement (mm²) of coloured pixels. Distinction was made between superficial and deep intratendinous flow, and flow in Hoffa's fat pad. Relative flow density (mm² flow/tendon thickness) also was calculated.

Clinical evaluation was based on the VISA-questionnaire. Pearson correlations between numerical data, and Spearman correlations with ordinal VISA-data were performed with the statistical package SPSS 9.0.

Results

In proximal patellar tendinosis (n = 73) flow was demonstrated in 87% (average 18.2 mm²/SD 16.2). Between the flow parameters and VISA-items not a single statistically significant correlation could be demonstrated. The correlations between other parameters and VISA-items were between tendon thickness and item 2 (walking downstairs)(r = -0.235, p<0.05), item 3 (r = - 0.292, p<0.05), item 8 (painscore during sport)(r = -0.262, p<0.05), and the total VISA-score (r = -0.254, p<0.05); between the transverse diameter of tendinosis and item 1 (r = - 0.251, p<0.05), and item 2 (r= -0.300, p<0.05); and between the length of tendinosis and item 3 (full active non-weight bearing knee extension) (r = -0.238, p<0.05).

Conclusions

Although the presence of neovascularisation in symptomatic patellar tendinosis is high, it seems unrelated to jumping capability and painscores during sport. This strengthens the idea that neovascularisation is just one of the expressions of tendinosis. Among the US-detectable signs of proximal patellar tendinosis, tendon thickness is the only one to correlate with 3 VISA-items (including pain during sport), as well as with the total VISA-score.

THE USEFULNESS OF ULTRASOUND IN THE ASSESMENT OF ACUTE ACHILLES TENDON RUPTURE

S David, S Ostlere*

Department of Radiology* and Trauma and Orthopaedics
John Radcliffe Hospital Oxford UK

Purpose

To determine the usefulness of preoperative ultrasound in acute Achilles tendon rupture.

Materials and Methods

This is a retrospective study of 42 patients (28 men, 13 women) with acute Achilles tendon rupture who underwent pre treatment diagnostic ultrasound. The ultrasound reports were analysed and the site of rupture, distance from distal insertion and width of the tendon gap in neutral and equines positions were documented. Patients underwent operative treatment (percutaneous or open repair) or immobilisation in a cast on the basis of the ultrasound findings and clinical criteria. The rerupture rate and other complications were recorded over a minimum period of 6 weeks following completion of treatment.

Results

The mean age of the study group was 40 (range 31-77yrs). The site of rupture was located at an average of 5.7 cm from distal insertion. 21 patients underwent operative treatment (10 open, 11 percutaneous) and 21 conservative treatments in serial cast, depending upon clinical criteria and ultrasound findings. An average gap of 1.8 cm was found in patients who underwent open repair compared to 1.1cm undergoing percutaneous repair. Although ultrasound criteria were not the solitary factors in determining management, those tears with small (< 0.5mm) or no gap on equines were treated conservatively in nearly all cases. The complications in the operative group were 5% with numbness in 2 patients and superficial infection in one. In the non-operated group 3 patients suffered persistent pain. None of the patients suffered recurrent rupture.

Conclusion

In this study, using a combination of ultrasound and clinical criteria there was a zero rerupture rate at six weeks after completion of treatment. This compares with rerupture rates of up to 30% that have been recorded in the literature in study populations that have been randomly allocated to conservatively treatment. When used in conjunction with clinical assessment ultrasound is a useful technique in acute Achilles rupture.

ULTRASONOGRAPHIC EXAMINATION OF ACHILLES TENDON IN THE ITALIAN RUGBY TEAM PLAYERS

S Parodi, P Spagnolo, R Pastorino, M Falchi, E Silvestri, G Garlaschi

Purpose: to compare US imaging of Achilles tendon in rugby players (group 1) and in a control group (group 2) same age and gender but sedentary individuals.

Material and Methods: 35 professional rugby players, male, and 20 healthy subject underwent US examination. A mobile US machine (Sonosite) with a 10 MHz probe was used. The evaluation of Achilles tendon was performed bilaterally in prone position with 90° degrees flexed ankle. At third medium level, AP and LL diameters were measured. Moreover the inner structure of the tendon was examined.

Results: the thickness of Achilles tendon was significantly larger in athletes than in the control group: mean value AP= 6.4mm/5.7mm; LL=16.1/12.8 respectively. In 15% of group 1 abnormalities were found in tendon inner structure as fragmentation of fibrillar echostructure (9%) and hypoechoic areas (7%) and indicate a tendinosis condition. These abnormalities were mostly bilateral; when monolateral they were more frequent in the dominant side. In 4% were found small calcifications at the attachment tendon level.

Conclusion: the increase of thickness, hypoechogenic areas and calcifications are significantly more frequent in group 1 professional rugby players than in group 2 sedentary healthy individuals. Our aim is to follow-up this athletes in a longitudinal study to identify useful factors for an early diagnosis in asymptomatic condition (primary prevention) and therefore determine suitable preventive measures (physiotherapeutic program) .

USEFULNESS OF ULTRASONOGRAPHY IN THE DIAGNOSIS OF CARPAL TUNNEL SYNDROME

I Pinilla, C Martín-Hervás, D Bernabéu, S Santiago*, G Gómez-Bajo**.

Departments of Radiology, *Neurophysiology and ** Plastic Surgery. Hospital Universitario La Paz. Madrid. Spain

PURPOSE: the aim of this study is to determine the usefulness of sonographic measurement of the median nerve for the diagnosis of carpal tunnel syndrome (CTS), as well as its correlation with the electrophysiologic examination in a case-control study.

MATERIAL AND METHODS: twenty-nine wrists of 17 patients (16 female, 1 male, mean age: 53 years, SD 13) with clinically diagnosed moderate-severe CTS and 22 wrists of 11 healtht controls matched for sex and age were studied. Sonographic examination was performed with a 7.5 MHz linear-array transducer (Siemens) in both, patient and control groups. Measurements of the cross-sectional area and anteroposterior diameter of the median nerve were obtained immediately proximal to the carpal tunnel inlet and immediately distal to the carpal tunnel outlet. Patients underwent further evaluation with electrophysiological study. Sonographic measurements of the median nerve were compared with the distal motor and sensory conduction velocity of the median nerve.

RESULTS: the mean median nerve cross-sectional area at tunnel inlet was 9.26 mm^2 (1.40-17.12, CI 95%) for the patients and 4.20 mm^2 (1.46-6.94, CI 95%) for the control group ($p < 0.001$); the mean anteroposterior diameter of the median nerve at carpal tunnel inlet was 2.21 mm (1.35-3.07, CI 95%) for the patients and 1.92 mm (1.42-2.42 CI 95%) for the control group ($p = 0.03$), the median nerve cross-sectional area at tunnel outlet was 7.45 mm^2 (1.37-13.53, CI 95%) for the patients and 4.27 mm^2 (1.88-6.66, CI 95%) for the controls ($p = 0.001$); and the mean anteroposterior diameter of the median nerve at carpal tunnel outlet was 1.92 mm (0.68-3.15, CI 95%) for the patients and 1.89 mm (1.58-2.20, CI 95%) for the controls ($p = 0.849$). No significant correlation was found between the ultrasonographic measurements of the median nerve and the electrophysiological parameters. Eight patients have already been operated with surgical confirmation of the CTS and marked clinical improvement.

CONCLUSION: the ultrasonographic measurement of the cross-sectional area of the median nerve at the carpal tunnel inlet and outlet, as well as the anteroposterior diameter at the tunnel inlet are useful parameters for the diagnosis of CTS, without correlation with the electrophysiological findings.

PERCUTANEUS MANAGEMENT OF CHRONIC CALCIFIC TENDINITIS OF THE SHOULDER

R Zabala, JL del Cura, A Legórburu, I Torre, A Garcia, D Grande

PURPOSE:

Percutaneous treatment of painful shoulder related to calcific deposits within the rotator cuff tendons.

PATIENTS AND METHODS:

We have studied 38 patients (25 females and 13 males), with chronic symptoms of painful shoulder resistant to medical treatment.

All of them had radiographically and ultrasonographically verified calcific tendinitis .

Percutaneous fine-needle aspiration and lavage under ultrasonography control, was performed in 38 patients.

We had used 20 gauge needle and 2% Lidocaine. At the end of the treatment, local steroid injections was performed in the bursa, using 40mg. of Depomoderin.

The protocol we had used, was:

- Medical evaluation of the shoulder by using the Shoulder Pain and Disability Index (SPADI) questionnaire. The SPADI questionnaire measures functional status of the shoulder.
- Aspiration of the calcifications.
- Injection of steroid.
- Radiography and ultrasonography controls were performed a week, a month and two months after.
- Medical evaluation (SPADI) two months and a week after the percutaneous treatment.

RESULTS

In radiographics, calcified deposit disappeared in 23 cases, decreased in 11 and no difference was seen in 4 patients.

By clinical evaluation, 14 patients were asymptomatic and in 15 cases the pain decreased. There was clinically significant improvement in disability score in 18 patients.

CONCLUSION:

Needle aspiration of the calcifying tendinitis of the shoulder is a useful treatment to improve the symptoms of painful shoulder for a short time. Calcified deposit disappeared in some cases. It is a cheap therapy. But, it is still necessary to follow up the patients during longer terms and performed comparative studies with other techniques.

THE USE OF ULTRASOUND GUIDED ASPIRATION / BIOPSY IN SPINAL PATHOLOGY

JM Elliott, AC Grey, RI Davis

Department of Radiology, Musgrave Park Hospital Belfast

Department of Histopathology, Royal Group of Hospitals Belfast

Purpose. To describe an ultrasound guided biopsy technique to aid in the diagnosis of spinal pathology.

Method and Materials. Eight patients (4 males, 4 females) with MRI findings of a mass or fluid collection involving the posterior elements or paraspinal tissues were examined sonographically using either Acuson or Diasus equipment with 3.5MHz, 7MHz, 5-10 or 8-16 MHz transducers. In each case the lesion was localised by ultrasound and its solid or cystic nature determined. Using real-time guidance, core biopsy or aspiration was performed as appropriate. The tissue or fluid was submitted to Histopathology or Bacteriology laboratories for diagnosis.

Results. In two patients Staphylococcus Aureus was cultured. In one of these patients infection was centered on the sacro-iliac joint and in the other involved a facet joint with extension into the epidural space. The other diagnoses were osteochondroma of the thoracic spine, neurofibroma, chordoma and three cases of metastatic carcinoma. There were no complications. Further management was aided in the instigation of appropriate antibiotics/surgery in the infectious cases and surgery / radiotherapy in the tumours.

Conclusion. Ultrasound guided biopsy offers a safe accurate method of obtaining a diagnosis in lesions of the spine that have a substantial paraspinal involvement or associated soft tissue fluid collection.

ULTRASOUND-GUIDED PERCUTANEOUS NEEDLE THERAPY OF THE ELBOW EPICONDYLITIS

M. Obradov, D. Eygendaal, P.G. Anderson, M. Reijnierse
Department of Radiology, Department of Orthopaedics, Orthopaedic Research, Sint Maartenkliniek, 6522 JV Nijmegen, The Netherlands

Purpose: The aim of this pilot study is to assess the effect of the ultrasound-guided needling of the chronic lateral or the medial elbow epicondylitis combined with corticosteroid injection in the group of the patients that are not responding to a previous conservative or surgical management.

Materials and Methods: Included in this study, performed from May through October 2003, were 25 consecutive patients (M: 10; W: 15; mean age: 41,7) visiting orthopaedic outpatient clinic with chronic medial (10) or lateral (15) epicondylitis. Mean duration of complaints was 24 months. All of them had concordant pain, previous corticosteroid injection, physiotherapy, 7/25 brace and 8/25 surgery. An ultrasound investigation with a phased array linear transducer (5 MHz to 12 MHz) showed erosive cortex lateral 7/15 (46,7%), medial 4/10(40%); hypochoic tendons lateral 7/15 (46,7 %), medial 5/10(50%); relative same incidence of the tendon calcifications: lateral 11/15 (73,4%), medial 9/10(90%); primary tear lateral 4/15 (26,7%) medial 5/10(50%). The clinical effect of needling was considered a success if patients had an excellent Andrews test ((Elbow functional assessment), decrease of the VAS score for at least three points, improvement of the "grip strength" and complete restoration of the work and sport activities.

Results: Twelve-week follow-up showed a statistically significant reduction ($p = .001$) of the VAS score laterally during provocation (a mean VAS score before/after: 7.53/3.43). Total 8/25 patients (all with lateral epicondylitis) completed all criteria of clinically successful needling. All of them subjectively feel a complete restoration of the elbow function and they are satisfied with the procedure. In the whole group there was no significant difference in the incidence of tendinosis, tendon calcifications, positions and aspect of dimensions of the calcifications. The whole group had predominantly involvement of only m. extensor carpi radialis brevis (5/8) and 7/8 had no previous surgery.

From total 8 patients with previous surgery 5/8 showed no change in the "grip strength", 7/8 no changes in the Andrews test and 6/8 no change in the VAS score. The "failure" group (only patients without previous surgery) of 10 patients consisted of 8 patients with medial epicondylitis and 2 patients with lateral epicondylitis. 6/10 had primary tendon tear and both cases of lateral epicondylitis showed simultaneous involvement of the m. extensor carpi radialis longus and brevis.

Conclusion: On the basis of the pilot study results we decided to start prospective crossover investigation (needling + corticosteroid + anaesthetic versus corticosteroid + anaesthetic) on patients with chronic lateral epicondylitis and without previous surgery.

Use of Curavisc in knee disorder – Ultrasound report

Biljana Djokic,

Department of Radiology, Health Service Nis, Bratislav Stankovic, Orthopedic and Surgical Department, Health Service Nis

The aim of work: Ultrasound account changes on disorder knee before and after application Curavisc (Hyaluronic acid). Hyaluronic acid is fluid due to presence in the synovia of all joints particularly in the large weight bearing joints where it endures normal painless movement due to its lubricating and shock absorbing. Moreover it is responsible properties for the nutrition of the cartilage. In degeneration joint disorder such as osteoarthritis synavial fluid is significantly reduced. Joint destruction of the cartilage increases followed by pain and restricted mobility of the affected joint.

Supplementation of synavial fluid by intra-articular administration of Curavisc containing of sodium hyaluronade may ameliorate the viscoelastic properties of Synavial fluid.

Material and methods: In last period of one year on Department of Radiology Nis, 150 patients with pain, cedema and reduced mobility of knee joints were various age and sex.

All patients were diagnostic by X-ray and ultrasound diagnostic.

On plain film are seen cortical changes. Ultrasound examinations were made with probe 7.5 – 10 MHz (Partner AU3 Esaote BioMedica).

Parameters for diagnostic protocol were:

- diameter of articular calrtilage
- absence or presence sinavilis, bursitis
- bone erosion
- changes on soft tissue (tendinitis, entesitis)

Results: All patients had reduction of diameter, cartilage (measured on femur cordila) - 1.2-1.8mm, erosion of surface caritilage – 125 patients.

198 patients had bursitis in one or more bursa.

57 patients had changes on tendons and ligaments.

Bone erosion had 47 patients (osteofila and erosion).

After application of 3-5 injection (usually 3) we saw better results:

- pain and mobility were better in 80% of patients
- diameter of articular cartilage were 1.6-2.2 mm (in 65% of patients after 6 months)
- all patients had reduced tendinitis and bursitis

Conclusion: In our small experience Curavisc is a medical device of choice at patients with degenerative and other articular disorders. Ultrasound is primary and the best diagnostic method in evaluation of use Curavisc in disorder knee.

RHEUMATOID ARTHRITIS: ASSESSMENT WITH CONVENTIONAL RADIOGRAPHY

Franz Kainberger

Department of Diagnostic Radiology, Medical University of Vienna, Austria

Rheumatoid arthritis is a systemic inflammatory disease affecting the synovium and other parts of joints as well as connective tissue in general. Conventional radiography of the hands, the feet and other painful joints has been, despite significant advances in imaging with US and MRI, defined as primary imaging investigation technique for early diagnosis and for follow-up studies. Assessment of the severity of joint damage by means of radiography has become a definite part of deciding the initiation of treatment and of control of therapy. Demands to quantify the severity of disease raised even further with new drug regimens. Proper investigation techniques in a standardized manner are indispensable for defining joint space narrowing or the size of erosions with sufficient reproducibility. Factors influencing the precise evaluation, i. e. limitations of image quality, advanced stages of the disease with malalignment, or surgical procedures have to be recorded. Image interpretation includes assessment of soft tissue swelling, joint space width, the size of erosions, and mutilation. Several techniques of scoring exist in various modifications. The Larsen scoring system has been established as a standard in Europe, whereas a system developed by JT Sharp and its modifications by H Genant and D van de Heijde have been used extensively in North America. Scoring is the more precise the more parameters are measured and calculated, thus increasing the amount of time to investigate the images. Therefore, attempts have been made to develop semi-automatized techniques basing on simple calculation algorithms and on more advanced image processing systems.

Radiologists should become familiar with the established techniques of quantification of arthritis as well as with recent advances in computer-assisted devices.

THE EULAR-OMERACT MRI IN RHEUMATOID ARTHRITIS REFERENCE FILM ATLAS – A NEW TOOL FOR STANDARDIZED ASSESSMENT OF RHEUMATOID JOINT INFLAMMATION AND DESTRUCTION

M. Østergaard¹, P. Bird², F. McQueen³, B. Ejlertsen¹, J. Edmonds², M. Lassere², C. Peterfy⁴, P. O'Connor⁵, R. Shnier², H. Genant⁴, P. Emery⁵, P. Conaghan⁵.

¹Copenhagen, Denmark, ²Sydney, Australia, ³Auckland, New Zealand, ⁴San Francisco, United States, ⁵Leeds, United Kingdom.

Purpose: To develop a standard reference film atlas for MRI-scoring of inflammatory and destructive changes in the hands and wrists of patients with rheumatoid arthritis (RA).

Methods: Based on a previously developed RA MRI scoring system (the OMERACT 2002 RAMRIS), the original development team agreed on the joints, MRI features, MRI sequences and image planes that would in their opinion best illustrate the scoring system in an atlas. After collecting several (≥ 3) representative examples of each grade, the team met for a 3-day period to review the images, and choose by consensus the most illustrative set for each feature, site and grade. A predefined subset of images (e.g. for erosions: all coronal slices through the bone) was extracted. These images were then re-read by all observers to confirm the scores originally assigned. Finally, all selected images were photographed and formatted by one centre and distributed to all readers for final approval.

Results: Providing examples of every grade of every feature for every bone in the wrist and metacarpophalangeal (MCP) joints was considered unnecessary and excessive. Examples were limited to the following:

Synovitis (Score 0-3):

MRI-sequences: Axial T1-weighted before and after i.v. gadolinium-contrast injection;
Anatomical sites: a) MCP-joints: 3rd MCP joint; b): Wrist: Radioulnar, radiocarpal and intercarpal joints.

Bone erosion (Score 0-10):

MRI-sequences: Coronal + axial T1-weighted;
Anatomical sites: a) MCP-joints: 3rd phalangeal base, 3rd metacarpal head; b): Wrist: 3rd Metacarpal base, capitate, scaphoid, lunate, triquetrum, radius.

Bone edema (Score 0-3):

MRI-sequences: Coronal T2-weighted fat suppressed or inversion recovery (STIR).

Anatomical sites: As for erosion.

A total of 1050 images were selected and mounted on individual sheets to allow easy use as standard references during review of other images.

Conclusion: An EULAR-OMERACT reference image set for MRI-scoring of RA of the hand and wrist was developed. This makes it possible to score MR-images for inflammatory and destructive changes according to the best possible match with standard reference images, similar to the method used for Larsen scoring of radiographs. This may improve the consistency of MRI scoring among different centres and different studies.

MAGNETIC RESONANCE IMAGING IDENTIFIES SUB CLINICAL FEATURES THAT PREDICT EXTENSION OF ARTHRITIS IN CHILDREN WITH OLIGOARTHRITIS

K Johnson , J Gardner-Medwin*, CAJ Ryder,

Birmingham Children's Hospital and Glasgow University* United Kingdom.

Introduction

Most children with oligoarthritis who have juvenile idiopathic arthritis (JIA) do well, but a significant number have a more aggressive disease course. Identifying those children at risk of developing more arthritis at presentation would help guide prognosis and management. We examine if magnetic resonance (MR) imaging is more sensitive than clinical assessment at identifying those at risk of extending arthritis to more joints.

Methods

Ten children (3 male, 7 female) with a mean age of 8.7 (5.5-14.3) years at first presentation of a monoarthropathy who were diagnosed as having JIA were recruited. The presenting joint was a knee (8), an ankle (1) and elbow (1). Joints with arthritis were recorded at presentation, and at a minimum of 6 monthly intervals over 3 (1-3) years by a blinded clinician. MR imaging of the clinically unaffected knee was performed at presentation, (8 MR within 1 month, 2 within 4 months) and reported by 2 blinded paediatric radiologists. The families were blinded to the MR results. Clinical management was dictated by the clinical findings.

Results

Six children had persistent oligoarthritis over the 3 years (1-3) of the study. Five had normal MR imaging, and one had an MRI scan reported as equivocal/normal. Four children clinically extended to develop arthritis in other joints over 2 years, all had abnormal MR scans at presentation. Two children developed clinical features in the previously normal knee, 4 months and 1 year after MR imaging first identified abnormalities in those joints. In the 2 other children their imaged knees remained clinically normal at the end of the study (2 and 3 years) but arthritis developed in other joints 2 and 7 months after the abnormal knee MR scans. The MR changes were synovial hypertrophy, lymphadenopathy and joint effusions.

Conclusions

MR imaging accurately predicted those patients who extended their arthritis. Imaging identified change in children's joints up to 1 year before this was clinically apparent. The results suggests a widespread inflammatory process may exist at presentation in children whose arthritis extends, and this has implications for our disease understanding, and the nature and timing of therapeutic interventions.

A PILOT STUDY FOR THE VISUALIZATION AND ANALYSIS OF ARTHRITIC CHANGES IN THE RAT KNEE JOINT BY MICRO CT ARTHROGRAPHY

^{1,2}F.W. Roemer, ^{1,3}A. Mohr, ¹J.A. Lynch, ¹M.D. Meta, ¹A. Guermazi, ¹H.K. Genant

¹Osteoporosis and Arthritis Research Group. Department of Radiology. University of California, San Francisco

²Department of Radiology, Klinikum Augsburg, Germany

³Department of Radiology. University of Schleswig Holstein. Kiel, Germany

Purpose: To evaluate the potential of the novel technique of micro CT arthrography for the assessment of arthritic alterations in the rat knee joint with adjuvant arthritis. Specific aims of the study were the visualization of osseous and chondral arthritic changes as well as of alterations of the intrinsic joint ligaments and menisci. Secondary aims were the structural analysis of the cancellous bone within the tibial epiphysis.

Material & Methods: 6 rat knee joints with either moderate (= group 1) or severe (= group 2) arthritic alterations on conventional radiography were evaluated using micro CT (0.125 mA, 40 keV, 30 μ m slice thickness, 30 μ m isotropic resolution, mean scanning time 3.0 hours). Arthrography was performed using a transpatellar tendon approach. For the micro CT evaluation multiplanar reconstructions were applied. Structural analysis of cancellous bone within the tibial epiphysis was performed and compared to the results of four control specimens without arthritis. The following structural indices were analyzed: Total Volume (TV), Bone Volume/Total Volume (BV/TV), Bone Surface Density (BS/BV), Trabecular Number (TbN), Trabecular Thickness (TbTh), Trabecular Separation (TbSp), Structure Model Index (SMI), Degree of Anisotropy (DA).

Results: Diffuse as well as focal cartilage loss could indirectly be visualized. Ligamentous or meniscal changes were not seen. Bony appositions and erosions were shown. Structural analysis of the tibial epiphysis showed marked abnormalities of all structural indices (mean values and standard deviations):

Group 1: TV 16.24(SD \pm 0.79) mm³, BV/TV 0.18 (SD \pm 0.02), BS/BV 21.2 (SD \pm 0.87)/mm, TbN 1.95 (SD \pm 0.15)/mm, TbTh 94.5 (SD \pm 3.9) μ m, TbSp 0.42 (SD \pm 0.04) mm, SMI 2.56 (SD \pm 0.18), DA 1.48 (SD \pm 0.13).

Group 2: TV 16.04 (SD \pm 1.11) mm³, BV/TV 0.07 (SD \pm 0.02), BS/BV 25.7 (SD \pm 1.8)/mm, TbN 0.94 (SD \pm 0.24)/mm, TbTh 78.1(SD \pm 5.3) μ m, TbSp 1.04 (SD \pm 0.31) mm and SMI 3.25(SD \pm 0.20) DA 1.36 (SD \pm 0.21).

Conclusion: Micro CT arthrography is suitable for the visualization of morphological arthritic alterations of cartilage and bone in the adjuvant arthritic rat knee. Additional important information about structural changes of cancellous bone can be obtained by structural analysis of the tibial epiphysis.

ACHILLES TENDON ENTHESOPATHY IN PSORIASIS: DIAGNOSTIC IMAGING WITH COMPARISON BETWEEN SONOGRAPHY, COLOR-DOPPLER AND MAGNETIC RESONANCE

F Maggi, F Di Gregorio, C De Simone
Università Cattolica del Sacro Cuore, Roma

Purpose: Identify ever earlier evidence of enthesopathy in arthropatic and non-arthropatic psoriatic subjects; compare the efficacy of Ultrasound and MRI in the evaluation of early signs of Achilles enthesopathy in psoriatic patients; evaluate the relevance of neovascularization using Color Doppler and T1-weighted sequences after administration of Gadolinium.

Materials and methods: 33 consecutive psoriatic patients, 26 men, 7 women, mean age 48 years (age range 19-72) entered the study. All patients underwent sonography of the Achilles tendon and peritendinous structures with Aplio (Toshiba) equipped with a linear multifrequency (8-13 Mhz) transducer; the study was completed with Color-Doppler analysis. An MRI study, before and after gadolinium, was then performed using E-Scan XQ (Esaote), 0,2 Tesla superconducting magnet. Axial and sagittal T1 and T2 weighted, sagittal GE and STIR sequences were obtained. After gadolinium, axial and sagittal T1 weighted sequences were obtained. The pathologic conditions documented with Sonography and MRI were classified into: acute tendinitis, degenerative tendinitis, paratendonitis, bursitis, rupture. Presence of vessels inside the tendon and signs of increased or abnormal vascularization in peritendinous structures were searched with Doppler and with sequences obtained after administration of Gadolinium.

Results: The more frequent US findings were signs of degenerative tendinitis (30% of cases) and signs of bursitis (33%); uncommon were signs of paratendonitis (12%). Microcalcifications, a sign of degenerative tendonitis, were found in 8 patients (24%). No acute tendinitis or rupture were diagnosed. Completion with Echo-Color-Doppler did not add significant

data to US study. In two cases, vascular signals were found inside the Achilles tendon; in one patient an abnormal vascularization was found in Kager triangle. MR imaging identified degenerative tendinitis only in 6 cases (18%), confirmed absence of acute tendinitis and ruptures and all the sonographic diagnosis of bursitis but two (27%), showed paratendonitis in 5 cases (15%). Microcalcifications were not identified in MRI study. All the alterations were identified in the basal study; no additional pathological finding and no evidence of abnormal vascularization were found after administration of gadolinium.

Conclusion: Most common disorders were degenerative tendinitis, in particular with microcalcifications as pathologic sign, and an unexpected high rate of bursitis; sonography represents a useful tool for an early diagnosis of Achilles enthesopathy while MRI, especially with low magnetic field, is not sensitive compared to US in detecting early changes in psoriatic patients; contribution of Color Doppler and of post-contrast MR images does not seem significant in this set of patients.

Magnetic resonance imaging in knees of patients with osteoarthritis at multiple sites: association with clinical findings

Peter R Kornaat, MD¹, Johan L Bloem, MD¹, Ruth YT Ceulemans, MD¹, Naghmeh Riyazi, MD², Frits R Rosendaal, MD³, Rob G Nelissen, MD⁴, Margreet Kloppenburg, MD²

¹Department of Radiology, ²Department of Rheumatology, ³Department of Clinical Epidemiology, ⁴Department of Orthopaedic Surgery, Leiden University Medical Center, Leiden, Netherlands

Objective: To determine the association between a spectrum of structural abnormalities found on magnetic resonance (MR) imaging of the knee and clinical findings in patients with familial osteoarthritis (OA).

Methods: MR images of the knee were obtained in 105 sib-pairs (210 patients) diagnosed with symptomatic OA at multiple sites. MR images were analyzed for the presence and severity of cartilaginous lesions, osteophytes, subchondral cysts, bone marrow edema, meniscal abnormalities, effusion and Baker's cysts. All patients were interviewed concerning the presence or absence of pain or stiffness in the imaged knee during the month prior to MR. Patients were randomized into two groups. Imaging findings with an odds ratio (OR) for pain or stiffness greater than 2 were identified in one group and subsequently OR's of these parameters were determined in the second group.

Results: Marked joint effusion is associated with pain (OR: 6.9; CI: 0.8-57) and stiffness (OR: 6.8; CI: 0.8-60). Presence of >5 osteophytes in the entire knee (OR: 3.6; CI: 1.5-9.1) and >2 osteophytes at the patellofemoral compartment alone (OR: 3.0; CI: 1.1-8.3) are associated with pain. Bone marrow edema at the femorotibial compartment (OR: 2.9; CI: 0.8-11) and presence of a central osteophyte (OR: 3.0; CI: 1.1-8.3) were associated with stiffness. All other imaging findings including cartilage destruction were not associated with pain or stiffness.

Conclusion: Only marked joint effusion, presence of >5 osteophytes in the entire knee, presence of central osteophytes and bone marrow edema in the femorotibial compartment were associated with pain and/or stiffness in the knee.

DIAGNOSTIC IMPACT OF HIGH RESOLUTION COMPUTED TOMOGRAPHY (HRCT) OF THE ELBOW

A. Mester, *L Nemeth, *T. Kakosy, *M. Posgay, K. Karlinger, E. Mako:

Semmelweis University, Faculty of Medicine, Department of Diagnostic Radiology and Oncotherapy, Budapest, Hungary *National Institute of Occupational Health, Jozsef Fodor National Centre for Public Health, Budapest, Hungary

Purpose of the study was finding evidences of morphological differences in-between occupational vibration-related osteochondritis dissecans (OD) of elbow versus usual degenerative changes of osteoarthritis (OA).

Patients and methods: In 20 of 81 mail workers with clinical hand-arm vibration syndrome both elbow joints were investigated. Control group of other 20 patients suffering from elbow pain without known occupational vibration exposure were compared. Both Plain film radiographies (PFR) and HRCT studies were used. Evaluation of images: first done by three independent readers, followed by consensus opinion. Staging: stage I.: subchondral bone resorption (radiolucent area), stage II.: subchondral semilunar demarcations with sclerotic rim, stage III.: extensive rim sclerosis with fragmentation, in some cases with replacement and loose bodies.

Results: In occupational vibration exposed elbow cases (40 joints of 20 patients) OD was evident by HRCT in 9 joints: in 19 foci, while radiography suggested only a suspicion in 14 cases. In 4 cases impact of PFR and of HRCT were equal. In one case PFR morphology finding was usual OA, but HRCT proved OD. Two loose bodies were only depicted by HRCT. No joint space narrowing occurred. In case of OA the PFR and HRCT had similar impact in 9 of 10 cases. Osteoarthritis occurred with extensive irregular subchondral sclerosis, and irregular narrowed joint space with large marginal osteophytes in the control group. Minimum duration of exposure to vibration was 5 years to get any HRCT findings.

Conclusion: Morphological symptoms of occupational vibration related osteochondritis dissecans are much safer, and earlier positive by HRCT versus radiography. The HRCT was superior versus PFR both in sensitivity and specificity. Method of HRCT offers high impact in differential diagnosis of OD versus degenerative OA changes. The decision about expelling and/or financial recompense can be supported by objective method. Cessation of exposure can help to prevent progression, if early enough done. By the law in Hungary OD has been recognised occupational disease, while osteoarthritis has not.

IMAGE QUALITY IN THE LATEST DEVELOPMENT OF DIGITAL RADIOGRAPHY: ASSESSMENT AND COMPARISON AT CR AND DR OF SMALL JOINTS

Loft L¹, Jurik AG¹, Rasmussen J², Jensen JJ¹, Egund N¹

Department Radiology R¹ and Department of Medico-Techniques²
Aarhus University Hospital, 8000 Aarhus C, Denmark

Purpose: To assess and compare the latest development of high resolution CR with “conventional CR” and DR in the imaging of small parts of the skeleton and also the efficacy of the imaging systems at decreasing radiation exposures.

Materials and methods: The latest products from three different companies were evaluated and the results compared with one DR system (Siemens, Vertix FD, 7.5 pixels/mm). The CR cassettes used, were 18x24 cm with a resolution of 10 pixels/millimetre and one product with 20 pixels/millimetre. Measurements of low-contrast, high-contrast sensitivity and spatial resolution were obtained using the Leeds X-ray Test Object TOR (CDR) placed on the film side of a 30 mm perspex plate (no antiscatter grid). FFD about 200 cm. Entrance surface dose was measured with an ionisation chamber and comparable doses were obtained by different FFD's. The starting dose/exposure (210 γ Gy) corresponded to a 100-speed film system (Kodak Lanex Fine screen, MIN-R) followed by exposures corresponding to 200, 400, 800 ... 6400 speed systems. Standard small skeletal part parameters/curves on both CR and DR were used. Also assessed was the image quality of radiographs of the hands and wrists of different patients at different exposures. Three observers were used in all assessments.

Results: The highest exposure accepted by DR corresponded to a 400-speed film system. The spatial resolution of the 10 pixel CR's varied between 3.15 and 3.55 line-pairs at 100 and 200 speed exposures and decreased to 1.25-2.0 line-pairs at a speed of 6400. The highest resolution of DR was 2.8 line-pairs and declined parallel to the 10-pixel CR's at reduced doses. The 20 pixel CR demonstrated 5 line-pairs at speed 100 and 200 and 2.8 line-pairs at speed 6400. The high-contrast sensitivity was 17.0 for the 20 pixel system and between 14.3 and 16.0 for the 10 pixel systems and DR at speed 100-400 and the difference was maintained at reduced doses. There were minor differences at the low-contrast measurements. Image quality of the phantom and patient examinations of the 20-pixel system were comparable or even more contrast detailed than that of a 100-speed mammography film system.

Conclusion: For a dedicated musculoskeletal department of radiology, the 20 pixel-CR system can replace the image quality of mammography film/screen combinations. Remaining products were not accepted for replacement. In paediatric radiography, the 20-pixel system may demonstrate advantages at reduced exposures compared to the 10-pixel system and DR.

Comparison of ionic and non-ionic contrast agents for contrast-enhanced MR imaging of proteoglycan depleted articular cartilage

E. Wiener, K. Wörtler, M. Settles, E.J. Rummeny

Purpose: To compare ionic (Gd-BOPTA (Multihance ®) and Gd-DTPA (Magnevist ®)) and non-ionic (Gadoteridol (Prohance ®)) MR contrast media for contrast-enhanced imaging of PG (Proteoglycan) depleted cartilage. Therefore the temporal and spatial tissue distributions of contrast agents in papain-treated and untreated bovine patella cartilage were compared.

Materials and Methods: MR studies were performed for each contrast medium with three fresh bovine patellae. To induce loss of PG, fresh specimens were placed in papain solution. Then, patellae were placed in 1:200 diluted contrast solutions and high resolution (slice thickness 2.5 mm, in plane resolution 300 µm) T1 weighted spin echo, T1-, T2-, and proton density (PD) parameter images were acquired on a 1.5 T scanner every 30 minutes for 10 hours. Signal intensity (SI) time-curves from different cartilage layers were calculated and compared with SI time-curves from untreated cartilage.

Results: PG depletion showed no significant changes in cartilage T1, T2, PD or cartilage thickness. With all contrast media (Gd-DTPA, Gd-BOPTA and Gadoteridol) MR signal intensity increase (decrease of T1 and T2) in papain-treated cartilage was significant higher than in normal cartilage. Maximum relative enhancement was reached much faster (within the first hour) in papain treated cartilage than in untreated cartilage. These effects depended on the depth of the cartilage layers and were most pronounced in superficial layers (about 1 mm) and less pronounced in the deeper calcified layers.

Conclusions: Gd-DTPA, Gd-BOPTA and Gadoteridol promised to be useful for contrast-enhanced cartilage imaging. Enhancement via diffusion is influenced by the molecular structure and charge of the gadolinium complex. In untreated cartilage, the negative charge of Gd-BOPTA and Gd-DTPA may cause a slower diffusion rate than the non-ionic complex of Gadoteridol. In PG depleted cartilage, loss of negative charges facilitates diffusion resulting in a higher concentration of contrast agent especially in superficial cartilage layers.

High Resolution Diffusion Tensor Imaging of Articular Cartilage

C Glaser*, L Filidoro*, O Dietrich*, T Oerther², M Witt², J Weber*, M Reiser*

*: Dept Clinical Radiology, Ludwig-Maximilians University Munich, Marchioninstr. 15, 81377 Munich, Germany

²: Bruker BioSpin GmbH, Rheinstetten, Germany

Purpose: In early osteoarthritis disruption of the cartilage's collagenous fibre network is regarded to be a hallmark of irreversible damage leading to further cartilage and joint degeneration. The purpose of the study was therefore to analyze microstructural properties of articular cartilage using diffusion tensor MR imaging.

Material and Methods: Human patellar cartilage-on-bone samples were imaged at 9.4T using a diffusion-w SE sequence (12 gradient directions, resolution: $39 \times 78 \times 1500 \mu\text{m}^3$). Voxel-based maps of mean diffusivity, fractional anisotropy and eigenvectors were calculated.

Results: Mean diffusivity decreased from the surface ($1.45 \times 10^{-3} \text{ mm}^2/\text{s}$) to the tide mark ($0.68 \times 10^{-3} \text{ mm}^2/\text{s}$). Fractional anisotropy was low (0.04 - 0.28) and had local maxima near the surface and in the lower third of cartilage. The eigenvector corresponding to the largest eigenvalue showed a distinct zonal pattern being oriented tangentially in the upper 30% and radially in the lower 60% of cartilage.

Conclusion: The findings correspond to current Scanning-Electron-Microscopy data on zonal architecture of cartilage. The eigenvector maps seem to reflect the alignment of the collagenous fibres as important structure giving component essential to the long term integrity of the cartilage matrix. In view of current efforts to develop and evaluate structure modifying therapeutic approaches, DTI may offer a promising tool for detection and follow-up of early cartilage damage in osteoarthritis.

IMAGING OF ADVANCED ARTICULAR CARTILAGE DISEASE USING 3D SPGR, 3D CISS AND PROTON FSE IMAGING AND ARTROSCOPIC CORRELATION

S Gur, R Arkun, S Aydogdu, M Argin

Ege University School of Medicine Department of Radiology

Purpose: To determine the accuracy of 3D SPGR, 3D CISS and proton density FSE articular cartilage imaging in the identification of grades 3 and 4 chondromalacia of the knee.

Materials and method: A prospective evaluation of 27 patients who underwent MRI and following 1-3 days arthroscopic evaluation was performed. The images were interpreted by an observer without knowledge of the surgical results. The medial and lateral femoral condyles, the medial and lateral tibial plateau, the patellar cartilage and trochlear groove were evaluated. MR cartilage images were positive if focal reduction (greater than % 50) of cartilage thickness was present (grade 3 chondromalacia) or if complete loss of cartilage was present (grade 4 chondromalacia). Comparison of the MR results with the arthroscopic findings was performed.

Results: 27 patients, 162 articular cartilage sites were evaluated with MRI and arthroscopy. Results of MR identification of grade 3 and 4 chondromalacia, all sites combined were: for 3D SPGR; sensitivity 85.3%, specificity 90.8%, positive predictive value 76%, negative predictive value 94.7% and overall accuracy 89.4% ; for 3D CISS : sensitivity 65%, specificity 90.9%, positive predictive value 76.4%, negative predictive value 89% and overall accuracy 86.4%; for proton FSE ; sensitivity 78.9%, specificity 91.9%, positive predictive value 75%, negative predictive value 93.4% and overall accuracy: 88.8%.

Conclusion: The results demonstrate that 3D SPGR, 3D CISS and proton FSE MR imaging can identify advanced chondromalacia. However, 3D CISS sequence is a new parameter for using cartilage imaging and seems is another useful sequence to image and evaluate for articular cartilage.

THE MEASUREMENT OF ARTICULAR CARTILAGE THICKNESS IN THE WRIST

Authors: C van der Leij, GJ Streekstra, S Strackee, M Maas.

Purpose: Thickness measurements of articular cartilage are clinically valuable in diagnosis of joint pathology. For example, they can be used to monitor the cartilage volume over time in osteoarthritic joint degeneration. Another area of use is the creation of a (patient specific) biomechanical model.

The objective of this study is to determine how the existing imaging methods for the detection of cartilage compare to the reality, and which method of cartilage detection and measuring for the wrist joint is optimal.

Materials and Methods: MR and CT acquisitions of three cadaver wrists were used for the cartilage thickness measurements, both with and without intra-articular contrast injection (a 1:1 mix of Hexabrix and Gadolinium). At four points, the cartilage thickness was measured. The routinely used MR sequence for the evaluation of cartilage (GE 1.5 T, FS-SPGR ($\alpha = 85^\circ$ TR=110ms TE min BW 41.87 SL 2mm)), and coronally reformatted CT images (Multidetector CT Philips MX8000, axial SL 0,5mm) were used for the thickness measurements. The obtained pictures were compared to images taken with a very high resolution digital camera (2000px * 2000px) of slices created with a cryomicrotome (slices every 100 μ m.), considered the golden standard. Signal magnitude plots perpendicular to the joint surface were created to get an impression of the cartilage thickness. This was accomplished first by hand, and later with a tailored computer program.

Results: Due to the pixel size of 0,31 mm of the chosen MRI sequence, only 5-10 points were measured for a signal magnitude plot, divided over two cartilage layers, two bone surfaces and the joint space. This combined with the blurring caused by the slice thickness, lead to inaccurate cartilage thickness measurements. The MR images with intra-articular contrast agent also showed artefacts.

The pixel size of the reformatted CT pictures was 0,2 mm, and the slice thickness 0,6 mm (Full Width at Half Maximum), which made them more useful for the thickness measurements. The automated thickness measuring method for the CT data showed an average absolute deviation from the golden standard of 25 percent, which is 0,2 mm with an average cartilage thickness of 0,8 mm.

Conclusion: CT images with intra-articular contrast injection are the most useful in our experiment. For further study, the use of other MR sequences and 3D data acquisition is recommended. For quantitative purpose, automated cartilage thickness measurements are advised.

CARTILAGE DAMAGE AND SYNOVIUM CHANGES IN HAEMOPHILIC ARTHROPATHY: EVALUATION WITH MAGNETIC RESONANCE IMAGING

Fotiadis NI, Girtovitis FI, Haritanti A, Dimitriadis AS, Makris PE.

Radiology Department and Haemostasis and Thrombosis Unit A' Propedeutic Clinic of Aristotle University of Thessaloniki, GREECE

Haemophilia is an X chromosome linked disease characterized by an increased tendency to hemorrhage mainly into joints. Due to recurrent haemarthroses specific changes occur in synovium and cartilage. This process is called haemophilic arthropathy. The aim of our study was to determine the value of magnetic resonance imaging (MRI) in the evaluation of early pathologic changes of haemophilic arthropathy.

We investigated 53 joints (27 knees, 14 elbows, 10 ankles and 2 shoulders) in 18 patients with Haemophilia A aged 5-57 years old (median age 21) which all had at least one episode of previous acute haemarthroses. In all patients plain film radiographs (anteroposterior and lateral) and MRI evaluation was performed when there was no clinical signs of acute haemarthroses. MRI protocol consisted of T1 SE, T2*GRE, T2 FSE and whenever necessary STIR in three perpendicular planes. We used intravenous contrast medium (Gadolinium DTPA) in only 3 cases to better delineate the hypertrophy of the synovium.

Synovial hypertrophy and hemosiderin deposition was detected with MRI in 36 patients, a finding with a very important role for the pathogenesis and evolution of the disease, and not detected with plain x-rays. Current concepts about the pathogenesis of haemophilic arthropathy, hold that the synovium becomes catabolically active because of the exposure to blood components and as a result induces cartilage destruction. Focal or diffuse destruction of the cartilage was observed in 27 joints with MRI while plain radiographs gave only indirect signs of cartilage destruction in 17 joints. Bony changes were equally well estimated with both methods.

In conclusion, we believe that MRI imaging, with specific sequences, is a non-invasive tool for the assessment of early joint cartilage and synovium pathological changes still undetectable by clinical examination or conventional X-rays in the haemophilic setting.

MRI IN MEMBRANOUS AUTOLOGOUS CHONDROCYTE IMPLANTATION (MACI)

E Fontoira, E Sánchez, M Padrón

Dept. of Radiology. Clínica CEMTRO. Madrid, Spain

PURPOSE: To describe the spectrum of MR imaging findings of chondral defects treated with MACI, including bone and cartilage expected changes and its complications.

MATERIALS AND METHODS: 42 patients (36 men, 7 women) with chondral defects underwent biopsy and transplantation of autologous cartilage using a porcine collagenous membrane instead of periosteum to cover the defect. This technique was used in 37 knees (one patient in both knees) and 6 ankles, from May 2002 until December 2003. Preoperative diagnostic and follow-up MRI studies were performed in a 1.5 T high-field strength magnet (GE Signa) using T1- and fat-suppressed proton density-weighted images.

RESULTS: MRI studies showed evolution of postoperative changes, with bone marrow resolution and signal changes in the implant. Images allowed us to evaluate the cartilage thickness and the articular congruency, and also possible complications as cartilage flaps or failure of the graft.

It also had a very good correlation with clinical outcome.

CONCLUSION: MR is an excellent imaging method to evaluate the postoperative evolution of chondral transplantation, as MACI

ARTHRO-MRI VIRTUAL ENDOSCOPY OF THE SHOULDER: PRELIMINARY RESULTS

M. Di Pietro, S. Lelli, V. Calvisi, A. Barile, C. Masciocchi

Department of Radiology, University of L'Aquila, Italy

Purpose. Aim of this work was to check Arthro-MRI virtual endoscopy diagnostic value in detecting shoulder pathology.

Materials and methods. 18 patients (aging 20-44) entered this study since September 2001 till September 2003. Arthro-MRI was performed employing whole-body units (GE 1,5 T) and a special softwear with SE T1 3D fat sat. We compared virtual MRI evaluation with arthroscopic findings.

Results. Arthro-MRI and virtual endoscopy showed 14 cases of antero-inferior glenoid labrum lesions and 4 cases of rotator cuff tear. Concerning rotator cuff tear, we were only able to perform virtual endoscopy of the bursae (enlarged by intra-articular contrast media). Neither false negatives nor false positives were discovered comparing Arthro-MRI, virtual endoscopy and arthroscopy.

Conclusion. We believe virtual endoscopy employing Arthro-MRI to be a worthy diagnostic method mainly in the evaluation of labral capsulo-legamentous injury due to shoulder post-traumatic instability. At present time virtual endoscopy does not add more informations for arthroscopic surgeons, if compared to Arthro-MRI. However, it allows a tridimensional view, which may represent a useful pre-surgical evaluation

Does marathon running cause stress on the knee, which is demonstrable on MR imaging?

Claudia Weidekamm, Martin Uffmann, Gerd Schueller, Till Bader

Medizinische Universität Wien / Universitätsklinik für Radiodiagnostik

Purpose:

The purpose of this study was to investigate whether running a marathon causes alterations of bone, menisci, ligaments, and/or cartilage that are demonstrable on MR images.

Materials and Methods:

Twelve non-professional marathon runners underwent magnetic resonance (MR) imaging of the knee before and immediately after running a marathon, using sagittal dual TSE-, 3D WATS-, coronal STIR, and axial T2-TSE-images. Two experienced radiologists interpreted the scans and graded the presence of lesions of menisci and cartilage on a 5-point scale, and bone marrow edema, ligamentous lesions, and joint effusion on a 3-point scale.

Results:

Bone marrow edema was neither present before nor after the marathon. In one runner, a punctate signal alteration in the anterior cruciate ligament was revealed after the marathon. Joint effusion was present in the pre-run scans of eleven out of twelve runners and increased slightly after the marathon. No cartilage defects were noticed.

Conclusions:

No cartilage lesions, bone marrow edema, and meniscal or ligamentous lesions were demonstrated on MR images. Joint effusion is a common finding in runners and increases by running a marathon.

MR 'ACCESSORY CLEFT SIGN' IN THE DIAGNOSIS OF GROIN PAIN.

PM Cunningham, D Brennan, J O'Brien, P O'Neill, S Eustace.

Department of Radiology, Cappagh National Orthopaedic Hospital, Dublin, Ireland.

Purpose: To describe an accessory cleft identified on coronal STIR images of the pelvis at the level of the symphysis pubis thought to reflect adductor avulsion at this site.

Materials and Methods: Fifteen sportsmen with groin pain referred for both symphysiography and MRI of pelvis were included for study. Patients were scanned on a 1.5 Tesla Philips gyroscan and subsequently underwent symphysiography.

Results: An accessory cleft was identified between the inferior pubic ramus and the adductor longus tendon attachment, extending to and communicating with the physiological cleft within the symphyseal fibrocartilage in each case. In each case the side of the cleft correlated with the side of symptoms. Coexistent osteitis pubis occurred in seven patients.

Conclusion: The MR accessory cleft sign is thought to indicate incomplete adductor avulsion in patients with groin pain. Its presence should be sought in groin pain sufferers and is likely to correlate with side of symptoms.

Polycystic Lipomembranous Osteodysplasia with Sklerosing Leukencephalopathy (Nasu-Hakola Disease) - 5 new cases –

J. Freyschmidt, A. Sternberg, J. Wiens, H. Madry

Purpose: To investigate the clinical and radiological findings and the follow-up of 5 new cases of polycystic lipomembranous osteodysplasia with leukencephalopathy (PLOSL). PLOSL is characterized by a combination of multiple bone “cysts” (especially in the ankles, wrists, feet and hands) with a loss of white matter in the brain (sclerosing leukencephalopathy), leading to presenile dementia. The disease is a genetically heterogenous disorder with a loss-of function mutation in the DAP 12 gene, with global distribution. The “cystic” bone lesions consist of fatty tissue with convoluted PAS-positive membranes.

Material and Methods: 2 brothers (38, 35 year old) and one sister (33 year old) with PLOSL, 2 other cases (males, 32 resp. 60 year old) with an unremarkable family history. From all patients the clinical, neuropsychiatric status, plain films from the wrists and hands as well as from the lower extremities, especially from the ankles and feet, MRI of the brain and in 4 cases MRI or CT of the affected bones were evaluated. In 3 cases an open biopsy was performed.

Results: At the first presentation 4 patients had pain in the affected bones, 2 spontaneous fractures. In a follow-up over a period of 10 years all patients developed spontaneous fractures, caused by the cystic lesions. At the first presentation the duration of the specific history ranged between a few months up to 10 years. Only 1 patient had neuropsychiatric symptoms at the first presentation, but all patients developed frontal lobe syndrome and presenile dementia during the 10 years follow-up. Neuroimaging disclosed abnormally high and progressively increasing bicaudate ratios and calcifications in the basal ganglia as well as increased signal intensities of the white matter on T2-weighted MR images. Well defined osteolytic (cystic-like) lesions with a sclerotic rim (diameter 0,5 – 3 cm) could be observed in the ankles, talar bones and other bones of the tarsus, metatarsals and phalanges as well in the wrists, metacarpals and phalanges of the hands. Number and distribution of the lesions varied from patient to patient. CT and/or MRI typically showed fatty content of the osteolytic lesions. One patient developed later on severe spontaneous fractures of cystic lesions in the femora, pelvis and spine.

Conclusion: PLOSL is a rare disease initially affecting the bones of the hands and feet and adjacent structures like the distal tibial epiphyses. Presenile dementia in all patients may develop in the early as well as in the late course of the disease. Most patients present with pain in the affected bones, possibly in combination with spontaneous fractures. The bony component of the disease may progress to a severe debilitating bone disease. The radiologic diagnosis can be made if CT and/or MRI demonstrate a fatty content of the “cysts”, that present as well defined osteolytic lesions (with diameters from 0,5 to 3 cm) with a sclerotic rim on plain film. Neuroimaging reveals signs of sclerosing leukodystrophy. The differential diagnosis includes cystic angiomas, sarcoidosis, Langerhans-cell-histiocytosis and unusual manifestations of non-Hodgkin-lymphoma of bone as well as peripheral multiple myeloma. Our observations are consistent with those in the literature.

NORA 'S LESION, A DISTINCT RADIOGRAPHIC ENTITY?

E.Dhondt¹, L. Oudenhoven¹, H. Kroon¹, A. Nieborg¹, P.Hoogendoorn², J.L. Bloem¹, A. De Schepper¹

¹Department of Radiology, LUMC, Albinusdreef 2, 2333 ZA Leiden, The Netherlands

²Department of Histology, LUMC, Albinusdreef 2, 2333 ZA Leiden, The Netherlands

PURPOSE: To describe the imaging findings of Nora's lesions (bizarre parosteal osteochondromatous proliferation) and to compare these data with findings on histological examination.

MATERIALS: Plain radiographs of 5 Nora's lesions out of a series of 100 consecutive cases of bone (pseudo)tumours of hand registered at the "Dutch Bone Tumour Committee", between March 2000 and December 2003. All cases were peer reviewed and histologically proven. Plain radiographs of all cases were available for study, together with MRI and CT in respectively 2 and one cases.

METHODS: Location and morphology on plain radiographs together with findings on MRI and CT were evaluated and compared with findings of non-Nora's lesions (95 cases). Radiological findings were compared with histological diagnosis.

RESULTS: Nora's lesions present as parosteal soft tissue calcifications with various morphological features. A radiological diagnosis of Nora's lesion was made in 3 out of 5 histologically proven Nora's lesions. In 2 of the remaining 95 cases an erroneous radiological diagnosis of Nora's lesion was made. The number of MR examinations was statistically non relevant.

CONCLUSION: Nora's lesions exhibit distinct histopathology and specific imaging findings. Diagnosis is mandatory to avoid aggressive workout.

Giant cell tumor of the tendon sheath of the hand: MR findings

S.Ortori, V. Zampa, S. Giusti, P. Vagli, F. Odoguardi, P. Alfieri, C. Bartolozzi

LEARNING OBJECTIVES: to describe the MR findings in patients with giant cell tumors of the tendon sheath (GCTTS) of the hand.

BACKGROUND: GCTTS can be divided in two different groups, the localized form and the diffuse form. The localized form of GCTTS of the hand involves particularly the flexor tendon sheath of the first three fingers representing the most common neoplasm of this region. It occurs at any age, but it is most frequent in women between 30 and 50 years old. Usually they are small (about up to 4cm), exophytically attached to the tendon sheath and their contour is smooth. The election treatment is surgery.

IMAGING FINDINGS: on MR GCTTS, is seen as well defined round or oval solid mass eccentrically located in relation to the tendon, or partially or completely envelopes it. On T1WI the signal intensity of GCTTS is usually similar or less than of skeletal muscle. On T2WI, although the lesion signal intensity is typically low, they may be varying degree of heterogeneity.

Marked contrast enhancement is often seen.

CONCLUSION: currently, MR is the modality of choice for the characterization and diagnosis of soft tissue masses of the hand. Moreover MR is a valuable modality for preoperative diagnosis of GCTTS.

THE VALUE OF THE "FLOW-VOID SIGN" ON MRI OF OSSEOUS METASTASES FROM RENAL CELL CARCINOMA

Allen G, Davies AM, Grimer RJ

PURPOSE: To assess whether the recently described flow-void sign (FVS) (Choi et al, Radiology 2003) is a frequent finding in patients with osseous metastases from renal cell carcinoma.

MATERIALS & METHODS: Two musculoskeletal radiologists retrospectively reviewed the MR scans of 17 patients in whom bone lesions in the appendicular skeleton, pelvis or scapula were subsequently histologically proven to be renal metastases. They assessed the images for the presence and frequency of the FVS - multiple low signal intensity dotlike or tubular structures due to prominent blood vessels.

RESULTS: The FVS was identified in 12 cases (71%) and was absent in 5 cases.

CONCLUSION: This study confirms that the FVS is a frequent finding in osseous metastasis from renal cell carcinoma. Identification of this sign may be helpful in directing appropriate further imaging in a patient presenting with an occult primary renal tumour.

WHOLE BODY MSCT VERSUS WHOLE BODY MRI IN DIAGNOSTICS OF MULTIPLE MYELOMA

A. Wieser, A. Baur, M. Reiser

Department of Clinical Radiology, University of Munich, Klinikum Großhadern, Marchioninstr. 15; D-81377 München

Purpose:

The aim of the study was to compare detection of bony involvement in whole body 16-Row-Multi-Slice-CT (MSCT) with whole body MRI in patients with multiple myeloma.

Patients and Methods:

20 patients with proven multiple myeloma were examined with whole body MSCT with a low-dose protocol (120 kV, 100 mAs, 1.5 mm collimation). The images were reconstructed in 3 mm axial slices and additional 3 mm sagittal slices of the spine. Whole body MRI was performed on a 1.5 Tesla system (Siemens Symphony) with coronal and sagittal STIR and unenhanced T1-w SE sequences. Two experienced radiologists evaluated CT and MRI blinded to clinical and histological data in a consensus reading. 44 anatomic regions per patient were evaluated.

Results:

Altogether 275 lesions were found either on MSCT and/or on MRI. 167 lesions typical for myeloma involvement were detected in CT as well in MRI. 88 lesions were detected exclusively on MRI, 20 lesions were exclusively detected on MSCT.

Conclusion:

Due to the direct visualization of bone marrow in MRI, early myeloma lesions can be detected exclusively in MRI if bony destruction is still lacking. Due to the high sensitivity of CT in depicting spongy structures, small osteolytic lesions were seen solely in CT.

Preoperative monitoring of neoadjuvant therapy in soft tissue sarcomas: The efficacy and limitations of MRI

A. Memis Oktay, R. Arkun, M. Argin, T. Akalin Y. Anacak, S. Arun

Medical School of Ege University, Department of Radiology, 35100, Bornova, Izmir, Turkey

Purpose: The objective of this study was to evaluate the efficacy of MRI in determining the response to preoperative radiochemotherapy of soft tissue sarcomas, and correlate the findings with histologic results.

Materials and Methods: 55 patients with soft tissue sarcomas were examined with conventional and dynamic contrast enhanced MRI before and after the neoadjuvant radiochemotherapy. Dynamic contrast enhanced MRI as obtained with SPGR/flash sequence (duration 20-40 sec) repeated 6-8 times after Gd-DTPA injection. The volume, SI characteristics and contrast enhancement pattern were evaluated, and the tumor necrosis were assessed. The percentage of necrosis on histologic examination and MRI results were compared.

Results: On histopathologic examination after the surgery, the response was good (necrosis above 90%) in 30 cases and poor (necrosis below 90%) in 25. The MRI findings were predicted the response in 47 cases, while in 8 cases the evaluation was false negative. The false negative results were seen in well differentiated liposarcoma in 3 cases, in mixoid liposarcoma in other 3, mixed liposarcoma in 1, and malign peripheric neurogenic sheat tumor in 1. The tumor necrosis could not be assessed in fatty tumors. The other limitation was seperated viable cells without any solid appearance.

Conclusion: MRI is an effective imaging modality in the evaluation of radiochemotherapy response in soft tissue tumors. This study demonstrated the limitations of MRI in assessing the response in well differentiated and myxoid liposarcomas.

BENEFIT OF PEER REVIEWED PATHOLOGICAL EXAMINATION OF SOFT TISSUE TUMORS, COMPARISON WITH RADIOLOGY?

JL Gielen, ADS De Schepper, F Vanhoenacker.

University and University Hospital of Antwerp, Belgium.

Purpose

The aim of the study is to objectify the benefit of peer reviewed pathology of soft tissue tumors and tumor-like lesions and to define the interaction between pathologist and radiologist.

Materials and Methods

Cases were selected from a multi-institutional prospective study on MRI of pathologically confirmed soft tissue tumors and tumor-like lesions. All cases histologically diagnosed as malignant were selected. Selected were also cases with discrepancy between biopsy and resection histology and lesions with indefinite histology results, and cases with discrepancy between histology and MRI. Six-hundred twenty-three cases have a confirmed diagnosis. Two hundred forty-four cases were selected for peer review following the above-mentioned selection criteria. Of 173 cases pathology slides are submitted to a peer review committee of 6 pathologists, specialized in soft tissue tumors. Three cases were excluded because of non representative biopsy, 67 of them were diagnosed as malignant, 103 tumors were benign. Biopsy and/or resection material were reviewed.

Results

Initial histological diagnosis is confirmed in 124 cases, 41 malignant, 83 benign lesions. In 26 malignant and 18 benign lesions histological diagnosis was refined or even changed. Histological phenotype changed in 10 benign and 11 malignant tumors. In four cases the initial malignant diagnosis changed into a benign one. In eight cases the initial benign diagnosis changed into a malignant one.

Discussion

In 44 cases (27%) the committee changed the histological diagnosis, in 15 (34%) the first or second MRI diagnosis is confirmed. Diagnosis changed in 26 (39%) out of 67 malignant lesions and in 18 (17,5%) out of 103 benign lesions. Diagnostic accuracy of the referral pathologist concerning benign lesions (82,5%) is obviously better when compared with malignant lesions (61%). Histological phenotype changed in 11 (16,5%) out of 67 malignant cases and in 10 (9,5%) out of 103 benign lesions. Because of therapeutic consequences cases with initially benign diagnosis which changed in a malignant one (8 out of 67) (false negatives) are of utmost importance, while the consequences of the vice versa situation (4 out of 103) (false positives) are not that significant. The accuracy of the referring pathologist in differentiating benign from malignant lesions is given in table 1, (CI: confidence interval at 95% confidence level using Walds method; + = malignant, - = benign). Peer reviewed cases Peer diagnosis + Peer diagnosis - Initial diagnosis + 59 4 93,5% PPV (CI 86.5-97.5) Initial diagnosis - 8 99 92,5% NPV (CI 85.5-96.5) 88% (CI 78-94) 96% (CI 90-99) 170 Total Sensitivity Specificity $p = <0.0001$ Table 1 Accuracy of the referring pathologist.

Fifty % (n=4) of the false negative cases (n=8) are lesions of lipomatous phenotype. In all 4 cases pathology (peer committee) confirmed the initial (differential) diagnosis made on MRI. Thirty three % (5 out of 15) of lesions in which the MRI diagnosis is confirmed by the peer review committee are lipomatous phenotype lesions. In 2 of these 15 cases the MRI diagnosis of myxoma is confirmed by the peer review committee, both of them have false positive pathology.

Conclusion

Discrepancy between MRI and pathology is an important selection criterion for pathological peer review optimizing the interaction between pathologist and radiologist.

CT ANGIOGRAPHY WITH VOLUME RENDERED THREE DIMENSIONAL IN PREOPERATIVE EVALUATION OF SOFT TISSUE TUMORS

L.Verga, A.Gallo, D.Martorano, V.Verna, A DeMarchi, C.Faletti.

PROPOSAL

Our aim was to assay the potentialities of CT angiography, in some cases with 3D reconstruction, in the evaluation soft tissue masses. Some information about the extension of closest vascular structure as high prognostic value were obtained and they could be considered as "milestone" for preoperative evaluation.

That's important because the vascular bundle involvement require a particular and different surgical approach.

MATERIAL AND METHODS

From November 2002 to February 2004 we studied 186 patients (aged from 22 to 85 years; mean 61) with soft tissue masses. All patients underwent ultrasonography and MRI study with and without contrast media.

After our studies, the histological controls were performed in all cases after MRI evaluation. We used a multidetector CT with 8 rows (Lighspeed Advantage CT-General Electric) with and without contrast media (Iomeron 400 mg/ml), analysing both arterial and venous phase. In all patients we obtained the multiplanar reconstruction (MPR) on sagittal, axial and coronal plane. In some cases (large mass and/or vascular bundle involvement) we completed the study with 3D reconstruction.

The patients were classified, in according to our orthopaedic surgeons, in two groups: 1) the tumor close to the main vessels without the vascular wall infiltration and 2) the malignancy involving and dislocating the vascular bundle, in order to plane the surgical approach.

RESULTS

104 patients had bundle involvement and 82 patients did not. We have studied in all the cases, in agreement with the orthopaedic surgeon, the dimensions and the connection with adjacent structures (infiltration and/or dislocation), showing also, in some cases, the three-dimensional images, to help surgeon planning the best approach to the lesion with particular regards to skin incision and to identify the lesion edges, for an accurate surgical strategy.

CONCLUSION

In the last few years the soft tissue tumors study has radically evolved and has been codified thanks to new clinical approach and new imaging techniques.

The interaction among surgeons, radiologists and pathologists allows adequate staging of soft tissue neoplasm and better planning for the definitive treatment. The spiral angio-CT with reconstructions gives a lot of very important information to the orthopaedic surgeon in evaluating and planning the best surgical procedures.

SOFT TISSUE TEMPERATURE CHANGES DURING CT-GUIDED RADIOFREQUENCY ABLATION OF OSTEIOD OSTEOMAS

Karl Ludwig¹, Ludger Bernd², Rüdiger Rupp², Rudi Georg Bitsch²

¹ Section of Diagnostic Radiology, Department of Orthopedic Surgery, University of Heidelberg

² Section of Oncology, Department of Orthopedic Surgery, University of Heidelberg

Purpose: Assessment of temperature changes in the soft tissue surrounding bone during radiofrequency ablation (RFA) of osteoid osteomas using an ex vivo animal model.

Materials and Methods: Intracortical cavities resembling nidus formations were created experimentally in three fresh bovine long bone specimens that served as a model for an osteoid osteoma. Different thicknesses of the cortical bone lamella separating nidus and periosteum were chosen for each of the specimens (1 / 3 / 5 mm). The diameter of the nidus was equal in all specimens (6.6 mm). Three temperature probes were applied to the soft tissue surrounding bone in defined distances from the periosteum (1 / 5 / 10 mm).

Before RFA the thickness of the cortical bone lamella and the distances of the temperature probes to the periosteum were documented by CT for each of the specimens. Specimens were heated in a water basin to 37 °C. RFA was performed with a target temperature of 95 °C for six minutes. During RFA continuous measurements were performed simultaneously with the three temperature probes. No simulation of vessel perfusion was used.

Results: For a cortical bone lamella of 1 mm maximum temperatures of 69.1 / 51.3 / 42.5 °C were measured in 1 / 5 / 10 mm distance from the periosteum. For a cortical bone lamella of 3 mm temperatures of 59.2 / 46.5 / 41.1 °C and for a cortical bone lamella of 5 mm temperatures of 50.6 / 44.8 / 40.0 °C were measured in 1 / 5 / 10 mm distance from the periosteum.

Conclusion: In our ex vivo animal model of osteoid osteomas soft tissue temperature during RFA was shown to depend on the thickness of cortical bone lamella and the distance from the periosteum. In vivo temperature in the soft tissue can be assumed to be lower than that in our ex vivo model due to the cooling effect of blood flow. Our results demonstrate, that with a cortical bone lamella of at least 1 mm thickness, there is no severe risk of a nerve damage in distances of more than 10 mm from the periosteum.

THE POTENTIAL VALUE OF MR IMAGING IN THE SEATED POSITION: A STUDY OF 116 PATIENTS SUFFERING FROM LOW BACK PAIN AND SCIATICA.

T. Muthukumar¹, F. W. Smith², D. Wardlaw², M. Pope².

¹Robert Jones & Agnes Hunt Orthopaedic Hospital, Oswestry, UK, ²University of Aberdeen.

PURPOSE: The clinical symptoms of lumbar spinal stenosis are often posture related. The availability of Open “Stand-up” MRI enables images of the spine to be made in any posture. This study explores the potential of upright MRI scanning in neutral, flexion and extension in sitting and supine position of patients with low back symptoms.

MATERIAL & METHODS: 116 patients [45 female & 71 male] (Age 35 – 71 years, mean 44 years), suffering from low back pain and/or sciatica were studied. Each examination was performed using a 0.6Tesla Open “Stand-Up” MRI. (FONAR, Melville, NY.) MR Images were obtained in both the supine and seated positions. Sagittal & axial T1 and T2 weighted were obtained in the supine, seated neutral, seated flexed and extended positions.

RESULTS: Measurements from “Normal discs” show changes of only 1mm in disc height between supine and sitting, increasing to 2 – 4mm reduction in height anteriorly on forward flexion and between 2 - 4mm reduction in height posteriorly on extension. Measurements from “Degenerate discs” show 1 – 3mm change in disc height between supine and sitting and significant reduction in disc height and position on flexion and extension.

108 prolapsed discs showed reduction of posterior prolapse on forward flexion & increase in extension, whilst 23 showed a decrease in posterior prolapse on extension.

In 21cases, the presence of a Grade 1 spondylolisthesis, not evident in the supine examination, was demonstrated in the seated position. In all cases, a degree of instability was demonstrated in the flexion and extension views.

In 4 cases of sciatica experienced whilst seated, in which the supine examination showed no abnormality, transforaminal disc herniation was demonstrated in the seated position.

CONCLUSION: We believe that the ability to image in the seated position is a major advance in the examination of the lumbar spine, especially in those patients with spondylolisthesis and position dependant disc prolapse.

PERCUTANEOUS VERTEBROPLASTY FOR THE TREATMENT OF OSTEOPOROTIC VERTEBRAL COMPRESSION FRACTURES AND SPINAL COLUMN NEOPLASMS

Kupes K, Aksiks I, Dzelzite S, Karklins E, Vestermanis V.

P. Stradins University Hospital, Riga, Latvia

Purpose. To evaluate the efficacy and pain reduction of percutaneous vertebroplasty in patients with osteoporotic compression fractures and spinal column neoplasms.

Materials and Methods. A total number of 35 patients and 59 vertebrae were treated with percutaneous vertebroplasty over a 2 year period. There were 19 women and 16 male patients. Their ages ranged from 18 to 82 years. 16 patients have osteoporotic compression fractures, 6 patients in multiple levels. 9 patients have symptomatic vertebral hemangiomas, 7 patients have metastasis from different origin, and 3 have multiple myeloma. For 14 patients multiple levels were treated simultaneously, up to 4 in one session. Approach was bipedicular in six cases, paravertebral in one and monopedicular in remaining. All cases were performed in one hospital. Polymethylmethacrylate (PMMA) was injected in a semi-solid state under fluoroscopic guidance into the vertebrae.

Results. All cases showed high technical success. After procedure pain reduction in visual analog scale (VAS) was from 8,6 to 2,9 points for patients with osteoporotic compression fractures, from 9,1 to 4,7 in patients with metastasis and 6,3 to 2,2 in patients with symptomatic hemangiomas. After two procedures epidural PMMM leakage was found without any clinical consequences. In one case subcutaneous hematoma developed after procedure.

Conclusion. Percutaneous vertebroplasty is a safe and effective minimally invasive procedure. Ensures good pain relief for patients with osteoporotic compression fractures and spinal neoplasms.

Transarterial Embolization for hypervascular bone tumor with use of superabsorbent polymer microspheres (SAP-MS)

Katsuyuki Nakanishi MD (1), Keigo Osuga MD (2), Shinichi Hori MD (3) Kenichiro Hamada MD(4), Nobuhito Araki MD(5) Takafumi Ueda MD(4), Hideki Yoshikawa MD (4) and Hironobu Nakamura MD (2)

(1)Department of Radiology, Osaka Seamen's Insurance Hospital (2)Department of Radiology, Osaka University Medical School (3)Gate Tower Institute for Image Guided Therapy (4)Department of Orthopedic Surgery, Osaka University Medical School (5)Department of Orthopedic Surgery, Osaka Medical Center for Cancer and Cardiovascular Diseases

PURPOSE: The purpose of this study is to evaluate the efficacy and safety of transarterial embolization (TAE) of hypervascular bone tumors with use of a spherical embolic agent, superabsorbent polymer microsphere (SAP-MS).

MATERIALS & METHODS: SAP-MS is characterized by calibrated microsphere without toxicity, which absorbs fluids resulting in tight vessel occlusion. Seven cases with malignant tumors (osteosarcoma 1, metastasis from renal cell carcinoma (RCC) 3, hepatocellular carcinoma (HCC) 2 and gastric cancer 1) underwent preoperative TAE (Group1; M:F=4:3, age=42-73yo, mean 63.3yo). Three cases with giant cell tumors (GCT) and eighteen cases with malignant

tumors (osteosarcoma 2, angiosarcoma 1, Ewing sarcoma 1, metastasis from HCC 5, RCC 4, thyroid ca. 2, alveolar soft part sarcoma 1, colon cancer 1, uterine cancer 1) underwent TAE with use of SAP-MS for symptom palliation (Group2; M:F=11:10, age=24-75yo, mean 61.4yo). The particles with smaller to middle size (53-106, 106-150, or 150-212 μm) were used in the aim of peripheral embolization of intratumoral vessels and increasing tumor ischemia. No chemotherapeutic agent was used in all patients. Radiation therapy and surgical resection was combined after TAE in three cases. Embolic effects were evaluated by intraoperative blood loss volume and the histological findings in Group 1, and the pain relief and its duration in Group 2.

RESULTS: In Group 1, intraoperative blood loss volume ranged 350 to 4150 (median 1225ml). Histological study revealed SAP-MS particles penetrated deeply into intratumoral vessels and occluded the vessel lumen tightly with minimal perivascular reaction. No inflammatory reaction was seen in the surrounding soft tissues. In Group 2, pain relief was obtained in 17 patients (81%). Pain relief lasted more than 40 months in two cases of GCT, and one to 41 months (mean 8months) in malignant cases. Transient neurogenic bladder was seen in a case.

CONCLUSION: SAP-MS particles were used safely in TAE of hypervascular bone tumors based on their inertness and calibrated spherical feature. Preoperative TAE using SAP-MS facilitated subsequent surgical excision of resectable lesions with minimal surgical morbidity, and provided good symptom palliation in cases with unresectable lesions.

Radiofrequency ablation in the palliative treatment of soft tissue tumors

Hoffmann RT, Schneider P, Reiser MF, Helmberger TK

Ralf–Thorsten Hoffmann, Institute of Clinical Radiology, University of Munich, Marchioninstr 15, 81377 Munich,

Purpose: To evaluate the efficacy of radiofrequency ablation (RFA) in the palliative treatment of soft tissue tumors causing pain or compression of adjacent structures.

Material and methods: Within 24 months RFA was performed in 18 patients with soft tissue tumors or metastases causing severe pain or compression of adjacent structures. 4 patients with pleuromesothelioma (3 malignant, 1 benign) and 14 patients with metastases of ovarian carcinoma (n=2), cervix carcinoma (n=2), breast cancer (n=4), renal cell carcinoma (n=2) or metastases of colorectal cancer (n=4) underwent treatment; the metastases were located in the mediastinum (n=1), in the psoas muscle (n=3), in the pelvic cavity (n=7), in the intercostal space (n=1) or next to the vertebral column (n=2). 7 patients suffered from a compression of either nervous or vascular structures. For tumor debulking we used three different RFA-systems. 14 patients were treated with the RITA system (RITA medical systems), two patients with the RTC–system (Boston Scientific) and another two patients with the Radionics system (Tyco Healthcare). Protocols were adapted from liver ablation protocols. To create a sufficient tumor necrosis we varied the number of positionings, the exact position of RFA probes and the duration of ablation. The clinical outcome was correlated with the degree of decompression and pain relief.

Results: Pain relief was achieved immediately after RFA in 16/18 patients; it lasted in 15/18 patients for up to 6 months. Decompression of nerves or vessels was possible in all treated cases.

Conclusion: RFA is a powerful tool to improve quality of life in patients with symptomatic soft tissue tumors by relieving pain of mass related symptoms in a palliative situation.

MYCOBACTERIUM BOVIS BCG OSTEOMYELITIS

K. Köllö, Gy. Szöke, T. Shisha, *A. Mester:

Semmelweis University, Faculty of Medicine, Budapest, Hungary

Department of Orthopaedic Surgery

*Department of Diagnostic Radiology and Oncotherapy

Purpose: Osteomyelitis, a rare complication after BCG vaccination can occur with a prevalence of 1/ 800 000. It is difficult the differential diagnosis in lack of imaging evidences of characteristic changes differentiating this form and sub-acute or chronic osteomyelitis. Authors analysed three cases, found during the past 20 years in Budapest, at the Semmelweis Uni. Department of Orthopaedic Surgery.

Patients and methods: Patients suffering from osteomyelitis confirmed by both clinical symptoms and radiological findings had laboratory tests, bacterial colonization from wound, mycobacterium specific studies, Mantoux test, immunological and histological tests. Age of patients was 8 month – 2 years. Only positive changes we got in rising erythrocyte sedimentation rate. Histology findings were specific to BCG osteomyelitis.

Results: The presentation is a pictorial assay about correlation of radiological studies and other documentations.

Discussion: Diagnostic problems are discussed in context of age of patients, anamnesis, diseases history, clinical symptoms and histology findings, which offer confirmation of suspected diagnosis of BCG-osteomyelitis. New methods of authors from Taiwan suggest application of DNS sequential analysis to get specific diagnosis to differentiate tuberculosis from BCG-osteomyelitis.

Conclusion: Rare complication of BCG vaccination can cause diagnostic difficulties. The complex clinical, radiological and laboratory approach, included genetic tests in the future could help the diagnosis.

WHITE CELL SCAN IN PROSTHETIC JOINT INFECTIONS

Munir U, Dussa C U, Herbert J

Purpose:

To see the accuracy of white cell scan in the diagnosis of prosthetic joint infections.

Materials and methods:

A retrospective study was done from Jan 2001 to Dec 2003 on patients with suspected joint infections after prosthetic replacements who had white cell scan. 67 patients were identified. We had excluded 8 patients due to lack of proper documentation. The case notes for clinical details, the laboratory investigations, radiological investigations were reviewed for this purpose.

Results:

After exclusion, of 8 patients, 59 patients who had white cell scan were taken into the study. Of these, 36 were males and 23 were females. The age range was from 53years to 91 years with an average of 72 years. We identified 21 total hip replacements, 33 total knee replacements, 3 shoulder replacements and 2 hemi-arthroplasties. 42 of these were cemented and 17 uncemented. The scan was done on an average of 23 months, with a range of 4 months to 16 years after the surgery. The chief complaint was pain in all patients. 5 patients had swelling, 1 had redness. None of the patients had discharge. White cells were raised in 1, ESR was raised in 5, and CRP was raised in 7 patients. Antibiotics were started on clinical grounds in 7 patients of which 5 patients showed no response. Plain X-Rays suggested infection in 5 patients. White cell scan suggested infection in 10 patients. Irrespective of scan report, 20 patients were operated for their symptoms. There was surgical evidence of infection in 10 patients and remaining 10 had aseptic loosening. Of the 10 surgically confirmed cases of infection, white cell scan showed infection in 6 patients. Scan negative patients were subsequently clinically followed and they did not show any infection.

	White cell scan +ve	White cell scan -ve
Infection present	6	4
Infection absent	4	45

The specificity of the WCS is 0.9 and sensitivity is 0.6. Likelihood ratio is 7.35. The confidence interval was 95%.

Conclusion:

White cell scan is a good investigation for confirmation of prosthetic joint infections. However caution should be excised in interpreting the negative scans. Persistent symptoms should not be ignored. Our study showed 6% false negativity. We recognise that the limitation of our study is our sample size

THE VALUE OF ULTRASONOGRAPHY IN THE DIAGNOSIS OF PYOMYOSITIS

E. Andipa, K.Bilas, V. Bizimi, P. Kolovou, K. Liberopoulos, M. Tsouroulas, G.Zois

Purpose of this study is to highlight the value of gray scale and color Doppler ultrasonography in the diagnosis of pyomyositis.

Materials and Methods. 9 patients 28-76 years old were referred to the ultrasound department due to the presence of pyomyositis. The muscles of arm, leg and thoracic wall were evolved. Ultrasonography was performed using a 5-12MHz transducer, as well as a convex transducer 2-5 MHz for deeper lesions. Color Doppler ultrasound was applied in all cases, while in 4 cases ultrasound contrast material (L-vist) was injected intravenously. US guided needle aspiration was performed in 5 cases.

Results. Ultrasonographic findings included oedema of the subcutaneous tissues, muscle enlargement, hypoechoic muscle appearance, fluid collection and abscess formation. Color Doppler ultrasound depicted increased vascularity in all cases. Thrombosis of the radial vein was depicted in one case. Contrast ultrasonography was very helpful in cases of abscesses (5 cases) strongly enhancing the increased vascularity and clearly demonstrating the ring-like vasculature around the abscesses. The cause of the disease was identified with aspiration and drainage was performed in 1 case.

Conclusion. Ultrasonography seems to be irreplaceable in the diagnostic and therapeutic work-up of pyomyositis. Not only, by means of color Doppler and enhanced ultrasonography, it can differentiate pyomyositis from other avascular entities, such as hematoma, and clearly depict the presence of abscesses, but it can also help by aspiration and drainage the therapeutic approach.

Infectious spondylodiscitis: (to) be (earlier) aware

Lange, C.A.H., Montauban van Swijndregt, A.D., Van der Woude, H.J. Department of Radiology Onze Lieve Vrouwe Gasthuis Amsterdam, The Netherlands

Purpose: To present plain radiographic, MR imaging and clinical features in a group of 25 patients with spondylodiscitis.

Patients and Methods: The imaging studies of 25 patients (mean age, 49 years (22-75 years)) with a diagnosis of spondylodiscitis on two or more levels (lumbar: 70%, cervicothoracic: 30%) between 1996 and 2003, were retrospectively analyzed by two radiologists in concert. Plain

radiographs (X) were compared with MR imaging studies, with emphasis on assessment of (loss of) vertebral height, decrease of disc space, extravertebral extension of the inflammatory process, features of the endplates and enhancement characteristics. Moreover, clinical indicators

and predisposing factors in this study group were evaluated.

Results: Loss of vertebral height was noticed in 42% of patients at the time of diagnosis. The endplates (X) showed lysis or mixed lysis and sclerosis in 85% at diagnosis. MR imaging revealed a heterogeneous pattern of the endplates on T2-weighted images, with contrast enhancement in 100%. Loss of disc space was present in 85% (X) and 88% (MRI), with complete disappearance of discs in 25%. Signal intensity of present discs on T2WI was increased in 58%, with suspicion of abscess in 39% of this subgroup. Enhancement of discs was

present in 69%. MRI demonstrated soft tissue extension in 75%, predominantly in the paravertebral, intraspinal and subligamentary space. The dural sac was compromised in 46% at time of diagnosis. Back pain was the main symptom in 92% of patients. Long-term duration of symptoms was present in 50% of patients (3 months - 2 years), intensifying in the final 1-3 weeks. In 80% of patients, the erythrocyte sedimentation rate was raised, with fever present in 33%. In 43% predisposing factors were manifest (alcohol abuse, HIV, TBC in the past).

Conclusions: The diagnosis of spondylodiscitis is frequently made in only an advanced stadium. Knowledge of (early) plain radiographic and diverse MR imaging features as well as clinical and predisposing indicators may probably direct to earlier detection and treatment.